

Invited Papers Presented To A Workshop On  
**THERMODYNAMICS AND KINETICS OF  
DUST FORMATION  
IN THE SPACE MEDIUM**

Houston, Texas  
6-8 September 1978

A Lunar and Planetary Institute Workshop



UNIVERSITIES SPACE RESEARCH ASSOCIATION  
LUNAR AND PLANETARY INSTITUTE  
3303 NASA ROAD 1  
HOUSTON, TEXAS 77058

INVITED PAPERS PRESENTED TO A  
WORKSHOP ON  
THERMODYNAMICS AND KINETICS OF  
DUST FORMATION  
IN THE SPACE MEDIUM

A LUNAR AND PLANETARY INSTITUTE WORKSHOP  
6-8 SEPTEMBER 1978

*Compiled by the  
Lunar and Planetary Institute  
3303 NASA Road One  
Houston, Texas 77058*

LPI Contribution 330



## TABLE OF CONTENTS

	PAGE
<i>Temperature fluctuations in interstellar dust grains</i> P. A. Aannestad and S. J. Kenyon	1
<i>Temperature parameters at condensation from the space medium</i> G. Arrhenius and J. L. McCrumb	4
<i>Sudden grain nucleation and growth in supernova and nova ejecta</i> D. D. Clayton	9
<i>Experimental techniques for the investigation of dust condensation processes</i> K. L. Day	12
<i>Disequilibrium thermal quasi-steady states in a cosmic dust cloud</i> B. R. De and G. Arrhenius	14
<i>Condensation in clouds: experiment and theory</i> B. Donn	17
<i>Time-dependent nucleation theory and the formation of interstellar grains</i> B. T. Draine	18
<i>A new model for interstellar dust</i> W. W. Duley, T. J. Miller, S. MacLean, and D. A. Williams	20
<i>Association reactions</i> E. Herbst	23
<i>Organic dust synthesized in reducing environments by ultraviolet radiation or electric discharge</i> B. N. Khare and C. Sagan	25
<i>Laboratory condensation of chondritic minerals</i> B. K. Kothari and J. R. Stephens	30
<i>Nucleation, growth and transformation of amorphous and crystalline solids condensing from the gas phase</i> E. Krikorian and R. J. Sneed	34
<i>The condensation and fractionation of Mg, Si and Cr</i> J. W. Larimer	38



<i>Grain carriers of isotopic anomalies</i> S. H. Margolis and S. W. Falk	40
<i>Dust in cosmic-plasma environments</i> D. A. Mendis	42
<i>The observed infrared properties of grains in space</i> K. M. Merrill	43
<i>Experiment on the clustering of fine particles</i> T. Onaka, Y. Nakada, and F. Kamiyo	45
<i>Computer simulation and the study of condensation</i> M. Rao and B. J. Berne	50
<i>Infrared studies of silicates</i> L. A. Rose	51
<i>Formation of H<sub>2</sub> on amorphous interstellar ice grains</i> R. Smoluchowski	53
<i>Effect of varied chemical composition, grain morphology, and chemical speciation on the 4-14 micron spectra of laboratory grain systems</i> J. R. Stephens	56
<i>The Allende meteorite: an assemblage of cosmic grains</i> D. A. Wark	59
<i>Recombination dynamics for H-atoms on surfaces of grains</i> W. D. Watson and D. A. Hunter	64
<i>Unidentified infrared spectral features</i> S. P. Willner, R. C. Puetter, R. W. Russell, and B. T. Soifer	65
<i>Ultraviolet scattering properties and the size distribution of interstellar grains</i> A. N. Witt	70

## INDICES

Subject index	72
Author index	74

TEMPERATURE FLUCTUATIONS IN INTERSTELLAR DUST GRAINS;  
P. A. Aannestad and S. J. Kenyon, Physics Dept., Arizona State  
University, Tempe, Arizona 85281

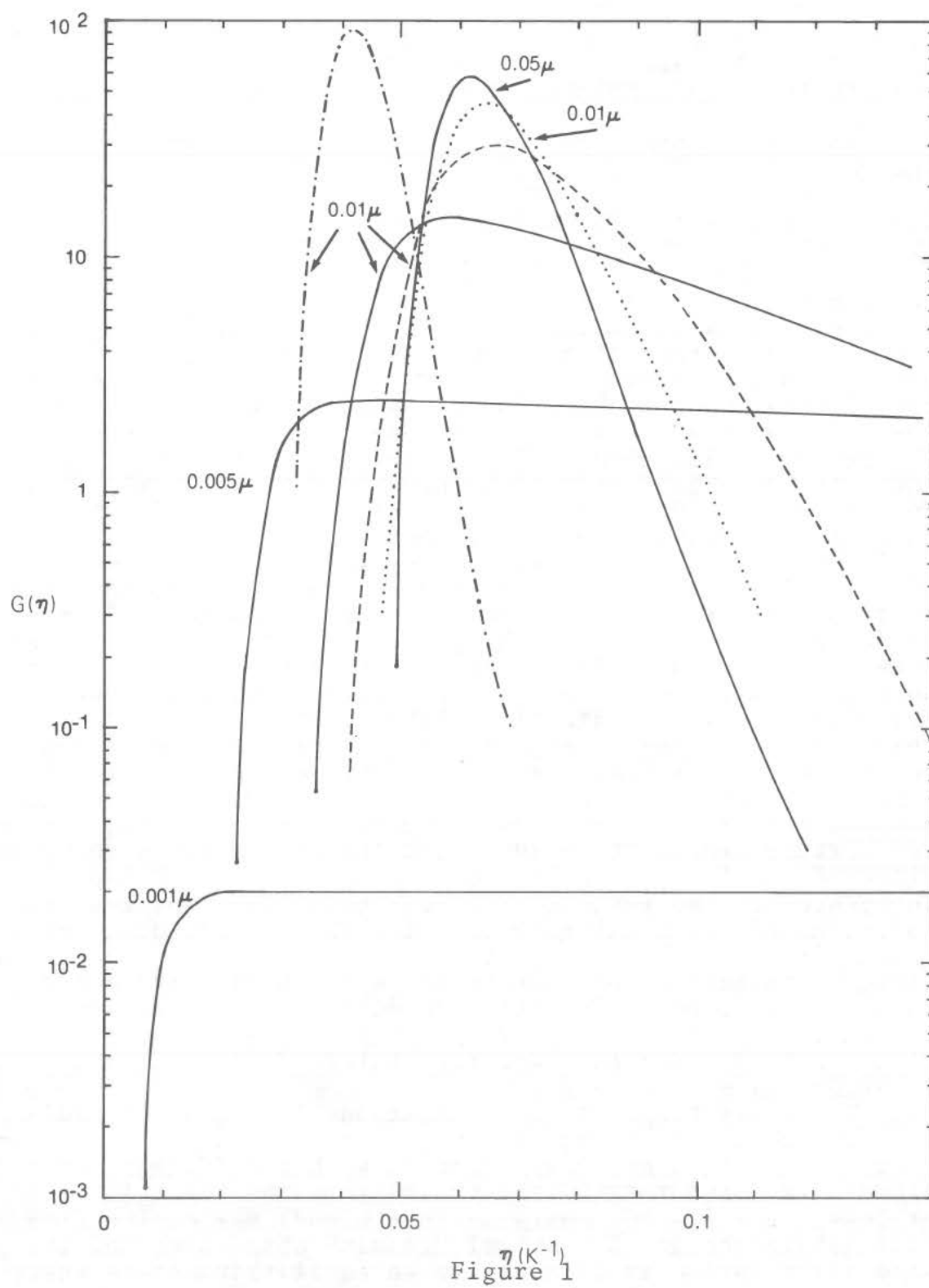
The heat content of interstellar grains with radii less than or about  $0.01\mu$  is small compared to the energy that may be deposited in the grains via photon absorption, bombardment by cosmic rays, or through molecular formation processes. Small grains thus undergo strong temperature fluctuations, and, depending upon the process considered, may not be adequately described by an equilibrium temperature.

We have extended the treatment by Purcell (1976) to consider grains larger than or equal to  $0.001\mu$  in radius that are exposed to the interstellar radiation field. Since the low-temperature approximation for the specific heat breaks down for the smallest grains, we have employed the full expression for the Debye specific heat. The dependence of the fluctuations on the infrared emissivity of the grain material has also been investigated. In addition, a high specific heat due to impurities at temperatures between 10 and 40K (Drapatz and Michel 1977) has been considered. Figure 1 shows the temperature distribution as a function of the inverse temperature  $\eta$  for various grain radii and assumptions about the thermal properties of the grains.  $G(\eta)d\eta$  is the fraction of time a grain spends between  $\eta$  and  $\eta+d\eta$ . The solid curves represent grains with a normal specific heat (Debye temperature 500K) and a far infrared emissivity  $\propto (\text{wavelength})^{-1}$ . Although the smaller grains reach relatively high peak temperatures ( $\geq 25\text{K}$ ), they spend most of their time at temperatures below about 10K; much lower than their equilibrium temperature of 15-16K. For grains of radius  $0.01\mu$  the dotted curve shows the effect of decreasing the Debye temperature from 500K to 200K, and the dashed curve shows the effect of employing a high specific heat caused by impurities. In both cases the range of the temperature fluctuations is decreased and is similar to that for the larger, but "normal" grains of radius  $\geq 0.05\mu$ . The dot-dash curve shows the temperature distribution for a grain of radius  $0.01\mu$  with a high specific heat, but a far infrared emissivity  $\propto (\text{wavelength})^{-2}$ . The smaller infrared emissivity makes this grain considerably hotter with an even narrower temperature distribution than the other grains of the same size.

The large temperature fluctuations in grains of radii  $\leq 0.01\mu$  may be important in inhibiting the small grains from accreting mantles of heavy elements within diffuse interstellar clouds. We find that if the photodesorption yield is about  $10^{-5}$  or less, in a few  $10^7$  years diffuse clouds may evolve from a state where the gas has normal "cosmic" abundances and the grain size distribution is unimodal to an equilibrium state where the

## TEMPERATURE FLUCTUATIONS

Aannestad, P. A. et al.



## TEMPERATURE FLUCTUATIONS

Aannestad, P. A. et al.

trace elements are depleted and the size distribution is bimodal.

Within dense and dusty interstellar clouds, where the temperature fluctuations due to the interstellar radiation field are decreased, heat input from  $H_2$  molecule formation on the grain surfaces may continue to prevent the small grains from accreting mantles, at least until the cloud is mostly molecular. In completely obscured regions with atomic hydrogen densities of about  $10^5 \text{ cm}^{-3}$  or higher, we find that grains smaller than  $0.01\mu$  cannot accrete material for which the adsorption energy is about  $0.1\text{eV}$  or less.

## REFERENCES

Drapatz, S. and Michel, K. W. 1977, Astr. Ap. 56, 353.

Purcell, E. M. 1976, Ap. J., 206, 685.



## TEMPERATURE PARAMETERS AT CONDENSATION FROM THE SPACE MEDIUM

G. Arrhenius and J. L. McCrumb, University of California, San Diego, La Jolla, California 92093

The average conditions under which molecular growth takes place in space are indicated by observations of dark interstellar clouds. These are, however, so remote that the critical inhomogeneities in density and state of excitation can not be resolved. Within our solar system direct measurements by space probes have given insight into the energetics and fine structure of the space medium. Condensation in the (atypically oxidizing) medium in near-earth space can be studied in meteor ablation plasmas and in the Junge particle layer in the Earth's upper atmosphere. Laboratory model experiments, appropriately scaling the properties of the space medium [1] provide additional insights. Reconstruction of primordial condensation associated with the formation of our solar system relies on this body of actual observation combined with analysis of relevant properties of solids surviving from the formative era (now mainly in certain types of meteorites).

The thermal properties of the source medium, i.e. interstellar gas, have to be distinguished from those of the condensing molecular aggregates growing into solid grains. In the source medium a number of different temperature parameters have to be defined; kinetic temperatures of electrons, ions and neutrals, and the temperatures associated with excitation and ionization. The thermal coupling of condensing grains to the source medium is highly dependent on the mode of condensation. If molecular growth takes place as a result of densification of the source medium at low average kinetic temperature ( $\sim 10^2$  K) as observed in interstellar clouds, the temperature of the grains may approach the average kinetic temperature of the medium.

If condensation were associated with radiative cooling of an initially warm ( $\sim 10^3$  K) cloud, grain growth would be practically limited to the peripheral regions with low optical depth, and the growing grains would necessarily assume a temperature much lower than the kinetic temperature of the source medium [3, 4, 5].

In a rapidly expanding hot medium ( $10^4$ – $10^6$  K) such as generated by stellar emission and explosion, the question whether condensation can take place or not during the expansion depends on the existence in each case of a cooling mechanism which is efficient enough to bring the medium into the thermal range of condensation before the density has fallen to such low values ( $< 10^6$  cm $^{-3}$ ) that supersaturation can prevail for long times (hours to years). The development of shock and critical velocity fronts, current filaments and electric double layers, such as observed in our region of space [6,7] are probably of major importance for damming up free expansion and increasing plasma densities to such levels that molecular growth can take place.

In preserved condensates, mostly from meteorites, that can be studied in the laboratory, it is easier to extract information on the thermal state of individual grains as they grew, than it is to find properties which reflect the complex thermal parameters of the source medium. Three major types of thermally activated phenomena can be drawn on to give direct information on the grain temperatures at formation. They are; allotropic phase transformation, diffusion phenomena, and chemical decomposition.

## Temperature Parameters

Arrhenius, G. and McCrumb, J.L.

Examples of transformation between high and low temperature minerals are  $\gamma \rightarrow \alpha$  nickel iron (1183°K for pure Fe), order-disorder transformations in metals (f.ex. PtNi at ~920°K) and silicates (such as pyroxenes, feldspars and probably in the melilite-åkermanite series) and magnetic transformations (f. ex. in magnetite,  $\text{Fe}_3\text{O}_4$  at 848°K).

Among diffusion phenomena that can be most easily exploited are those involving simple metallic systems protected against perturbing chemical effects. An example is given by the spherical platinum grains observed embedded in the interior of nickel-iron metal [8]. In this case (Fig. 1) the concentration of Pt diffused at time  $t$  to a radial distance  $r$  from the center of the original platinum sphere of size  $a$  is

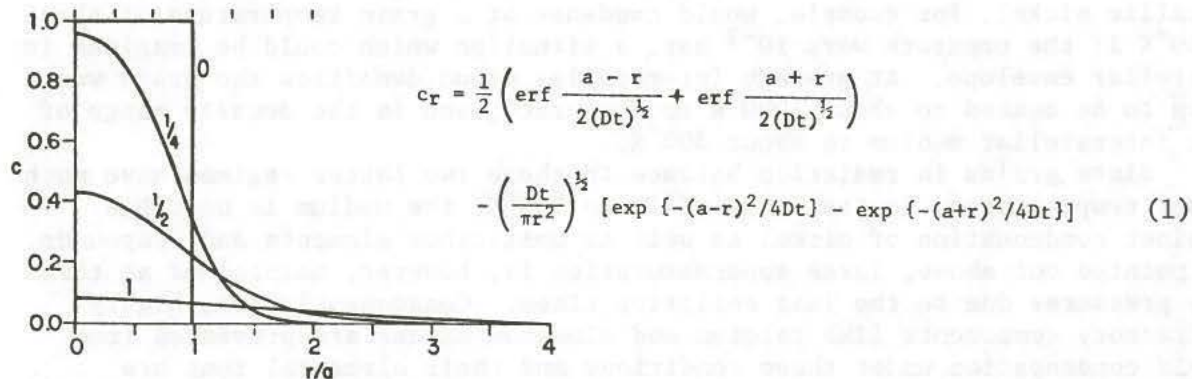


Fig. 1. Diffusion between a platinum sphere with radius  $a$  ( $\sim 0.6 \mu\text{m}$ ) and surrounding nickel iron metal. The concentration curves represent solutions of Eq (1) for the values of  $\sqrt{Dt}/a$  indicated. The upper radial scale is graduated in units of the experimental resolution limit [8] ( $0.2 \mu\text{m}$ ).

where the diffusion constant  $D$  is related to the temperature  $T$  by

$$D = D_0 \exp(-Q/RT) \quad (2)$$

and  $R$  is the gas constant,  $Q$  the activation energy.

Measurements of  $c_r$ , combined with values for  $D_0$  and  $Q$  which are well known for Pt-Ni consequently give direct information on the time during which any such diffusion couple can have been exposed to a given temperature. In the meteorites measured [8] the diffusion distance is below the limit of resolution ( $0.2 \mu\text{m}$ ), indicating [9] that the diffusion couple, if it was ever hot, could not have spent more than about an hour at 1000°K, or correspondingly longer time at lower temperature.

The nickel iron particles containing the platinum spheres occur in the interior of crystals of refractory minerals such as  $\text{MgAl}_2\text{O}_4$  (spinel), calcium aluminum silicate (melilite) and calcium magnesium aluminum silicate (fassaite pyroxene). The temperature-time limits imposed by the Pt-NiFe diffusion couples consequently place identical constraints on the grain



## Temperature Parameters

Arrhenius, G. and McCrumb, J. L.

temperatures at which the overgrowth by the refractory envelopes took place.

The irreversible exothermic transition from glass to crystalline state is yet another thermally activated diffusion phenomenon with potential information on the time-temperature exposure history of the grains [10].

The stability of solid phases against decomposition (and conversely, the stability of the source medium against condensation) gives a criterion for the upper limit of grain temperature at which a given phase could have grown, however, only under the condition that pressure, chemical composition and state of excitation of the source medium are known. Since these are observed to be variable over many orders of magnitude in the space medium and are rarely independently recorded in the solid condensates, it is difficult to make practical use of this information to determine grain temperatures. Metallic nickel, for example, would condense at a grain temperature of about 2150°K if the pressure were  $10^{-3}$  bar, a situation which could be imagined in a stellar envelope. At average interstellar cloud densities the grain would have to be heated to about 1000°K to evaporate, and in the density range of the interstellar medium to about 800°K.

Since grains in radiation balance in these two latter regimes have much lower temperatures, in the range of 10 to 100°K, the medium is unstable against condensation of nickel as well as most other elements and compounds. As pointed out above, large supersaturation is, however, maintained at these low pressures due to the long collision times. Consequently even highly refractory components like calcium and aluminum oxides are prevented from rapid condensation under these conditions and their elemental ions are observed in the interstellar medium. However, they are depleted relative to other elements, indicating that a substantial fraction has formed compounds, presumably with oxygen, at rates determined mainly by the collision frequency, and at temperatures far below the thermal stability limits of the solids. Other means for estimating upper temperature limits in this category are provided by volatile structural components of minerals, such as hydroxyl and halogen ions, and by inert gases occluded in defects in the growing grains. Such occluded noble gases in meteorite grains place particularly restrictive upper limits on the possible temperature of growth [11].

At the present primitive state of knowledge of the thermal characteristics including the state of ionization and excitation of the source medium it is difficult to separate, f.ex. ionization effects from other factors determining the observed properties of meteorite materials. This is partly because effects on the structure of the growing solid of even large excursions of individual temperature parameters of the source medium are subtle. In order to unravel the thermal properties of the medium from the record in meteorites, parameters in the solids have to be defined, which in a unique, unambiguous and model independent way reflect the state of the source medium. A possibility for characterizing the state of vibrational excitation and ionization of the source medium is provided by the non-linear fractionation in polyisotopic systems such as that of oxygen. The direct observation of very large kinetic two-isotope fractionation effects in microwave emission from interstellar clouds [12] make it likely that similar effects observed in meteorites [13] are due to such kinetic fractionation rather than to hypothetical regional differences in the isotopic composition of the space medium

## Temperature Parameters

Arrhenius, G. and McCrumb, J. L.

sometimes postulated to exist as a result of nucleosynthetic effects.

We are experimentally and theoretically exploring different molecular reaction mechanisms which a priori seem likely to cause non-linear isotope fractionation under space conditions, in order to determine their relative importance in this respect. Among these are particularly fractionation effects which are associated with isotopically selective Franck-Condon transitions from stable to repulsive states (predissociation) of excited molecules and molecular ions containing oxygen.

Choosing as an example the case (Fig. 2) where the crossover point  $E_c$  lies above the isotopic levels  $E_{16}$ ,  $E_{17}$  and  $E_{18}$ , (all with the same vibrational quantum number), the transition from the bound state  $U_b(r)$  to the repulsive state  $U_f(r)$  takes place by tunneling. The probability ratio for such predissociation from two different isotopic levels, f.ex.  $E_{16}$  and  $E_{17}$  can be shown to be

$$\frac{P_{16}}{P_{17}} = \left( \frac{\mu_{17}}{\mu_{16}} \right)^{\frac{1}{2}} \exp \frac{2}{\hbar} \left\{ \int_{r_{17}}^{r'_{17}} \left[ 2\mu_{17} (U(r) - E_{17}) \right]^{\frac{1}{2}} dr - \int_{r_{16}}^{r'_{16}} \left[ 2\mu_{16} (U(r) - E_{16}) \right]^{\frac{1}{2}} dr \right\} \quad (3)$$

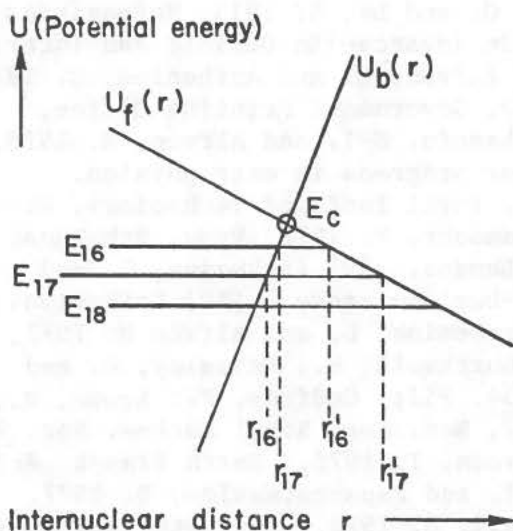


Fig.2. Region near crossing point  $E_c$  of a repulsive state  $U_f(r)$  on outer limb of potential energy curve  $U_b(r)$  for an excited bound state of  $^{16}O^{16}O$ ,  $^{16}O^{17}O$  and  $^{16}O^{18}O$ .

where  $\mu_{16}$  and  $\mu_{17}$  are the reduced masses of the isotopically different molecules, f.ex.  $^{16}O^{16}O$  and  $^{16}O^{17}O$ .

The integrals in Eq. (3) are thus functions of the areas bounded by the potential curves  $U_b(r)$  and  $U_f(r)$  and the respective isotopic vibrational energy levels  $E_{16}$  and  $E_{17}$ , and the probabilities are exponentially inversely proportional to the difference between the two integrals. It can easily be seen that the probability ratio is sensitive to the location of the crossover point relative to the isotopic vibrational levels, particularly when the slope of  $U_f(r)$  is small. The magnitude and the non-linearity of kinetic fractionation by predissociation in polyisotopic system (also in the classically allowed region) will thus depend on the energy of the crossover point relative to

## Temperature Parameters

Arrhenius, G. and McCrumb, J. L.

the vibrational energies and can not be accurately predicted. Instead it should be possible from model experiments combined with observations in space and in meteorites to deduce the specific state of excitation and ionization from which isotopically fractionating predissociation has taken place and thus to reconstruct these particular thermal characteristics of the source medium. The effects would be expected to vary in a non-systematic way between different molecular species. It is perhaps significant in this respect that large fractionation is seen in oxygen [13] and magnesium [14,15] with large nonlinearities only in oxygen while fractionation effects are much smaller and lack measurable accompanying nonlinearities in silicon [16] and calcium [17]. The assignment of specific molecular or ionic dissociation mechanisms for each isotopically fractionated reaction product in meteorites and in radiowave spectra requires extensive experimental work -- our present efforts concern reactions in the system CO-O<sub>2</sub> [18]. This system would appear to be of particular importance since related ions and molecules are observed to be the most abundant species next to hydrogen and helium in the interstellar cloud medium (cf. fig. 1 in [2]).

The present work is sponsored by grant NGS-05-009-002, from NASA's Office of Lunar and Planetary Science.

References: [1] Alfvén, H. and Fälthammar, C-G. 1963, *Cosmical Electrodynamics*, 2nd ed., Oxford Univ. Press. [2] Arrhenius, G. 1976, *Contrib. NATO Conf. Orig. Solar System*, Newcastle, England; in S. Dermott, ed., *Origin of the Solar System*, Wiley, NY, 1978. [3] Arrhenius, G. 1971, *Proc. Nobel Symp.* 21, 117, Wiley, NY. [4] Arrhenius, G. and De, B. 1973, *Meteoritics* 8, 297. [5] De, B. and Arrhenius, G. 1978, in *Advances in Colloid and Interface Science*, in press; also this volume. [6] Alfvén, H. and Arrhenius, G. 1976, *Evolution of the Solar System*, NASA SP-345, Government Printing Office, Washington, D.C. [7] Fälthammar, C-G., Akasofu, S-I. and Alfvén, H. 1978, *Significance of magnetospheric research for progress in astrophysics. Electron and Plasma Physics*, Report 78-07, Royal Inst. of Technology, Stockholm. [8] El Goresy, A., Nagel, K. and Ramdohr, P. 1978, *Proc. 9th Lunar and Planetary Science Conf.*, Pergamon Press, London. [9] Arrhenius, G. and Raub, C. 1978, *J. Less Common Metals*, Nov-Dec; in press. [10] Krikorian, E. and Sneed, R., 1978, this volume. [11] Arrhenius, G. and Alfvén H. 1971, *Earth Planet. Sci. Lett.* 10, 253. [12] Churchwell, E., Walmsley, C. and Winnewisser, G. 1977, *Astron. Astrophys.* 54, 952; Godfrey, P., Brown, R., Gunn, H., Blackman, G. and Storey, J. 1977, *Mon. Not. Royal Astron. Soc.* 180, 83 P. [13] Clayton, R., Onuma, N. and Mayeda, T. 1976, *Earth Planet. Sci. Lett.* 30, 10. [14] Wasserburg, G., Lee, T. and Papanastassiou, D. 1977, *Geophys. Res. Lett.* 4, 299. [15] Macdougall, D. 1978, *Proc. 4th Int. Conf. Geochron. Cosmochron. Isotope Geol.*, Snowmass, Colo. [16] Yeh, H-W. and Epstein, S. 1978, *Lunar Planet. Sci.* 9, 1289. [17] Russel, W., Papanastassiou, D. and Tombrello, T. 1978, *Geochim. Cosmochim. Acta*, August, in press. [18] McCrumb, L., Markus, S., Killingley, J. and Arrhenius, G. 1978, *Proc. 4th Int. Conf. Geochron. Cosmochron. Isotope Geol.*, Snowmass, Colo.

# SUDDEN GRAIN NUCLEATION AND GROWTH IN SUPERNOVA AND NOVA EJECTA,

Donald D. Clayton, Rice University (Houston) and Max-Planck-Institut für Kernphysik (Heidelberg, Germany).

Discoverers of isotopic anomalies concluded that carrier grains rich in  $^{22}\text{Ne}$  [1] and  $^{16}\text{O}$  [2] were grown in an anomalous synthetic pool. A stream of subsequent discoveries strengthens this idea, but has not clearly identified where and how fast the dust must grow. One possible scenario is that isotopically anomalous carrier grains will have been precipitated during the expansion of the supernova interior. We introduced this idea to try to account for the same  $^{16}\text{O}$  [3] and  $^{22}\text{Ne}$  [4] excesses in carbonaceous meteorite minerals. The condensation time scale should be about a year and begin about a year after the explosion, when the interior temperature has fallen from  $10^9\text{K}$  to  $10^3\text{K}$  and the density of newly synthesized refractory heavy elements to about  $10^{-14}\pm 2\text{g cm}^{-3}$ . This environment is optically thick, so the thermal radiation is in near equilibrium with the grain temperature. Many were quick to doubt that refractory dust particles can nucleate and grow at such low densities on this short (astronomically speaking) time scale. We emphasize two lines of evidence that it can. Both may be important to the physical understanding of dust formation.

The refractory elements Ca, Al, and Ti are known to be much more highly depleted from interstellar gas than are the refractory elements Mg, Na, and Si and the nonrefractory elements [5]. We have argued [6,7] that this comes about because the chemical composition of supernova shells, where these refractory elements first come into existence, are such that Mg and Si can only partially condense there whereas Ca, Al, and Ti must condense totally. The Mg and Si, coming largely from separate supernova shells, are unable to condense each other, but they (and O and S) are more than abundant enough to condense Ca, Al, and Ti. This abundance asymmetry offers hope of understanding how 99% of Ca, Al, and Ti reside in interstellar dust and may, with observational and theoretical strengthening, provide a proof that supernova condensates (SUNOCONS) are precipitated within the stellar interior itself. This line of evidence, though interesting and useful, is indirect.

A second and more direct type of evidence comes from common and observable nova explosions. The astonishingly rapid rise of infrared luminosity from Nova Serpentis (1970) [8] has stimulated us [9, 10] to formulate numerical models of the dust growth required to account for this infrared emission. Because the hot ( $\sim 50,000\text{K}$ ) central object is very luminous ( $L \sim 2 \times 10^4 L_{\odot}$ ), dust grains cannot form near it; otherwise they would quickly vaporize by heating to that temperature which balances absorption and emission from the grain:

$$\pi a_0^2 (L/4\pi r_0^2) \bar{Q}(T_*, a_0) = 4\pi a_0^2 \sigma_g T_g^4 \bar{Q}(T_g, a_0)$$

where  $a_0$  is the initial grain size a distance  $r_0$  from the central object and  $\bar{Q}$  is the absorption (or emission) efficiency. The former will be near unity as soon as the nucleating particles have been able to grow to  $a \sim 10^{-6}\text{cm}$ . Because very small grains absorb at  $T_*$  more efficiently than they emit at  $T_g$ , the grain temperature is greater than the equivalent temperature  $T_{\text{rad}}$  of a black sphere at that radius. For grains with  $a < 10^{-6}\text{cm}$  to form at grain temperature  $T_g$  ( $\leq 2000\text{K}$ ) requires that the distance  $r_0$  be great enough that the equivalent black-sphere temperature has fallen to approximately



# "NUCLEATION IN NOVAE"

Donald D. Clayton

$$T_{\text{rad}} \simeq 750^{\circ}\text{K} \left( \frac{a}{10^{-6}\text{cm}} \right)^{1/4} \left( \frac{T_g}{2000^{\circ}} \right)^{1.41}$$

so that a  $10^{-6}\text{cm}$  grain will fall below  $T_g = 2000^{\circ}\text{K}$  when  $T_{\text{rad}} < 750^{\circ}\text{K}$ . The definition  $4\sigma T_{\text{rad}}^4 = L/4\pi r^2$  shows that

$$r^2 = 2.6 \times 10^{40} T_{\text{rad}}^{-4} \quad (L = 2 \times 10^4 L_{\odot})$$

which has solution  $r > 2.8 \times 10^{14}\text{cm}$  for  $T_{\text{rad}} < 750^{\circ}\text{K}$ . Taking an expansion speed  $v = 700\text{ km/s}$  for the nova ejecta shows that a time  $t_0 = r_0/v = 4 \times 10^6\text{s} = 46\text{ days}$  is needed before  $10^{-6}\text{cm}$  grains could be as cool as  $2000^{\circ}\text{K}$  (i.e. exist). This delay is very nearly what was observed in Nova Serpentis 1970. Between days 55 and 60 after the outburst a hot infrared source began a rapid growth, after which the color temperature of the infrared radiation was slowly declining [8]. This behavior almost certainly measures the sudden growth of new grains when the temperature  $T_{\text{rad}}$  has fallen to a sufficiently low value. The infrared luminosity increases thereafter at the rapid rate of about 10% per day, which reflects the growing surface area of the grains as they deplete the condensible matter. A good match to observations is obtained [10] by assuming a high sticking fraction for atoms impacting the growing grains. The declining grain temperature between day 50 ( $\sim 1500^{\circ}\text{K}$ ) and day 90 ( $\sim 900^{\circ}\text{K}$ ), when  $L_{\text{IR}}$  reaches its peak, follows naturally from the increasing distance from the central object.

In such a rapidly expanding condition, grain growth ceases even without depletion of monomers. Assuming  $n(t) = n_0(t_0/t)^2$  as if undepleted monomers are confined to a spherical shell moving outward with constant thickness and constant velocity, we [10] found the grain radius

$$a = a_0 + 4 \times 10^{-20} t_0 \left[ 1 - (t_0/t) \right]^{5/4} n_0$$

starts from  $a_0 (\sim 3 \times 10^{-7}\text{cm})$  and grows to an asymptotic value  $a_{\infty} \sim 4 \times 10^{-20} t_0 n_0 = 1.6 \times 10^{-13} n_0$  for  $t_0 = 46\text{ days}$ . If the condensible mass ejecta is a typical value  $\sim 3 \times 10^{-4} M_{\odot}$  and if the shell thickness at  $t = t_0$  is  $10^{-2}$  of  $vt_0$ , then  $n_0 \sim 1.4 \times 10^9\text{ cm}^{-3}$ , yielding an asymptotic grain size  $a_{\infty} = 2.2 \times 10^{-4}\text{cm}$ . These choices agree well [10] with observation, causing  $L_{\text{IR}}$  to achieve maximum value at  $t_{\text{max}} = 1.91 t_0 \sim 88\text{ days}$  as observed. Nucleation would seem to concentrate on the earliest thermally permissible moments because of the rapidly falling density.

The success of this interpretation has important implications for grain nucleation and growth. With  $10^9\text{cm}^{-3}$  condensible particles, nucleation occurs rapidly, apparently within 10 days following the drop of  $T_g$  below  $2000^{\circ}\text{K}$ , whereafter grain growth occurs as rapidly as collisions permit. There is no more room to doubt that in stellar atmospheres grain nucleation can proceed quickly at density near  $10^9\text{cm}^{-3}$ . Interestingly enough,  $10^9\text{cm}^{-3}$  is also the density of O, Mg, Al, Si expected when the carbon shell in the supernova core has cooled below  $2000^{\circ}\text{K}$  [4]. The cooling rate and the density decrease are an order of magnitude slower in the supernova interior than in Nova Serpentis, however, so the nucleation and growth should be roughly "10 times easier" for the supernova than for Nova Serpentis. It is this reasoning that allows us to conclude

# "NUCLEATION IN NOVAE"

Donald D. Clayton

that Ca, Al, and Ti are depleted from the interstellar gas because they could not escape the supernova interior without condensing, primarily as  $^{16}\text{O}$ -pure oxides. Unfortunately, the chemical composition of Nova Serpentis is not well known. It was probably carbon-rich, but C/O may be either greater or less than unity, and contains H, unlike the supernova interior where H is absent.

A review of other novae [11] shows that some form dust and others do not; therefore, the novae as a class represent a common, but variable experiment in sudden dust production. Their borderline behaviour increases their value as an experiment. The trend is what one would expect; VIZ. the roughly ten-times-more-luminous "rapid" novae are not dust producers, probably because the higher luminosity reduces  $n_0$  by increasing  $r_0$  proportionally to  $\sqrt{L}$  and because a more rapid expansion allows less time for growth. Suppression of nucleation by ionization may also play a role [11]. Both theory and observation leave uncertainty in the range of nova chemical composition, however.

This work is supported in part by NSF and by NASA.

## References

1. Black, D.C. (1972) Geochim.Cosmochim. Acta 36, 377.
2. Clayton, R.N., Grossman, L., and Mayeda, T.K. (1973) Science 182, 485.
3. Clayton, D.D. (1975) Astrophys.J. 199, 765.
4. Clayton, D.D. (1975) Nature 257, 36.
5. Field, G. (1975) in: The Dusty Universe (G. Field and A.G.W. Cameron, eds.) Neale Watson, New York.
6. Clayton, D.D. (1977) Earth Planet.Sci.Letters 36, 381.
7. Clayton, D.D. (1978) The Moon and Planets (Protostars and Planets issue).
8. Geisel, S.L., Kleinmann, D.E., and Low, F.J. (1970) Astrophys.J. Letters 161, L101.
9. Clayton, D.D. and Hoyle, F. (1976) Astrophys.J. 203, 490.
10. Clayton, D.D. and Wickramasinghe, N.C. (1976) Astrophys.Space Sci. 42, 463.
11. Gallagher, J.S. (1977) Astron.J. 82, 209.



EXPERIMENTAL TECHNIQUES FOR THE INVESTIGATION OF DUST CONDENSATION PROCESSES. K. L. Day, Lunar and Planetary Laboratory, University of Arizona, Tucson, AZ 85721.

In this presentation I will discuss two laboratory methods by which we may gain information of use in the study of interstellar and circumstellar grains. While no laboratory method can exactly duplicate astronomical conditions, experimentation with condensation processes can be of considerable value. This is particularly true in light of the present state of the theoretical approach, in which the condensates are assumed to be well known terrestrial minerals.

At the Lunar and Planetary Laboratory of the University of Arizona, I have been exploring processes of surface condensation. This is a follow-up on the work of Myer (1) who condensed silicates in film form after producing vapor by radio-frequency sputtering of ceramic targets. The Arizona approach is somewhat different. I am doing DC sputtering of  $\text{MgSi}$  and  $\text{Mg}_2\text{Si}$  alloy cathodes. The sputtering chamber may be filled with a variety of reaction gases at pressure of 10-40 microns. To date I have used 50-50 argon-oxygen and 99% argon - 1% oxygen.

Atoms are liberated from the cathode in proportion to its composition, and these spread throughout the chamber, forming a thin film where they condense. They may react with oxygen on their flight or while they are still exposed, on the surface. A wide variety of astrophysically interesting compounds may be condensed this way.

While this method tells us little or nothing about the kinetics or detailed processes by which grains coalesce, it can shed light on subsequent growth and provides a wide variety of materials. There are several important advantages of the method just described. The target composition, ambient gas composition, substrate composition, and substrate temperature may all be closely controlled or known. Films may be grown at arbitrary speed to almost any desired thickness. Finally, the films themselves are nearly ideal for optical constants measurements and microprobe analysis as they are produced as very thin plane parallel slabs which require no polishing. Sticking coefficients and fractionation patterns are readily derived from the data, and the optical constants may be used in Mie calculations for comparison with astronomical data.

While much remains to be done with these experiments, some early results will be quoted here. I have produced silicate glass films with the compositions  $\text{MgSiO}_3$  and  $\text{Mg}_2\text{SiO}_4$ . Identical films were produced whether the oxygen content was 1% or 50% in the ambient atmosphere. My results do not confirm Myer's (1) observation of non-stoichiometric condensation at room temperature; the cation/silicon ratio in the condensed films was the same as in the target. Preliminary optical constants measurements in the infrared show that these films do not have very strong resonances near 10 microns, characterized by the real part of the dielectric constant going to -2, though it may go slightly negative. The infrared spectra of these glasses bear little resemblance to those of the terrestrial minerals

## Experimental Dust Condensation

K. L. Day

with the same compositions. They do bear close resemblance to various published astronomical spectra.

In collaboration with Dr. Bertram Donn of Goddard Space Flight Center I have also taken part in another series of silicate condensation experiments. The technique here is known as gas evaporation. We evaporate various cosmically abundant elements or compounds into inert or reactive atmosphere at a pressure of a few torr. At this pressure the mean free path length is on the order of microns. Thus the gasses are rapidly cooled to supersaturation and smoke particles precipitate directly from the vapor. These drift out on convection currents and are easily collected. By placing two or more independently controlled evaporation sources in close proximity, a common cloud of reactants is formed, and new compounds may form during the nucleation process. Some of these have been discussed in a recent publication by Day and Donn (2).

This method has several drawbacks. It is difficult to control the evaporation and mixing of constituent vapors and the particle morphology is neither easily controlled nor particularly amenable to microprobe analysis. However, the condensation of cosmically abundant vapors directly into free-standing smoke particles is reasonably well imitated by this process, so even if the variables are not completely controlled there is much to learn by observing the products. Plans for the future include further experimentation with both surface and smoke condensation procedures.

## References

- (1) Myer, C. Jr. 1971, *Geochim. Cosmochim. Acta*, 35, 551.
- (2) Day, K.L. and Donn, B.D. 1978, *Ap. J. Let.*, 222, L45.

# DISEQUILIBRIUM THERMAL QUASI-STEADY STATES IN A COSMIC DUST CLOUD

Bibhas R. De  
Lunar and Planetary Institute  
3303 NASA Road 1, Houston, TX 77058

Gustaf Arrhenius  
University of California, San Diego  
La Jolla, CA 92093

An isolated cloud of gas and dust in the otherwise relatively empty space (the intercloud medium) represents a thermodynamic system in which an equality - or even a near-equality - between the gas phase kinetic temperature  $T_k$  and the condensed phase (dust) internal temperature  $T_s$  hardly ever obtains [1,2]. In such clouds, thermal quasi-steady states [2] are possible where the rate of radiative heat loss of a dust grain is balanced by the rate of heat gain from the impacting gas molecules and the ambient radiation field. In the interior of the cloud, this radiation field is enhanced - especially in the infrared wavelengths - due to the radiation from the grains themselves. This enhancement causes the grains deep inside the cloud to be hotter than those near the cloud boundary. This depth-dependent temperature profile of grains was studied earlier under certain simplifying assumptions [3]. Here we present the outline of a more general study.

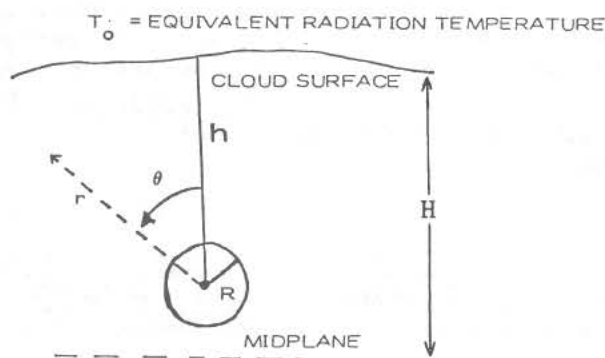


Figure 1.

Figure 1 is a sketch showing a dust grain located at a depth  $h$  below the freely radiating surface of a cloud which, for the purpose of illustrative calculations to be presented later, is assumed to be roughly disc-shaped with a midplane of symmetry. The definition of a cloud surface is of course always arbitrary - and we shall later avoid this arbitrariness by assuming that the gas density decreases linearly from a value  $N=N_0$  at the midplane to  $N=0$  at the surface. The gas is assumed to be entirely molecular hydrogen. Outside the cloud boundary, the temperature  $T_0$  characterizes the local radiation field - deriving from radiation from neighboring stars (but not the cloud itself). This temperature is defined as that which a blackbody in the region of the grain would attain if it did not receive any heat from the cloud. The grains, with a number density  $n(r)$ , are assumed to be all spherical blackbodies with radius  $a$ . Under these conditions, we find that the grain temperature at any point in the cloud is given by the convergent solution of the iteration relation:

## THERMAL DISEQUILIBRIUM IN COSMIC DUST CLOUDS

DE and ARRHENIUS

$$\sigma T_{s,(i+1)}^4 = \sigma T_0^4 + 2CNV k(T_k - T_{s,(i+1)}) + \frac{1}{2} \pi \sigma a^2 \int_0^\infty \int_0^\pi n(r) [T_{s,(i)}(r)]^4 \exp \left\{ - \int_0^r \pi a^2 n(r) dr \right\} \sin \theta \, d\theta \, dr \quad (1)$$

Here  $\sigma$  = Stefan-Boltzmann constant,  $k$  = Boltzmann constant,  $C$  = thermal accommodation coefficient,  $V = (kT_k/2\pi m)^{1/2}$  = average impingement velocity of the gas molecules ( $m$  = molecular mass), and the subscript  $i$  refers to the  $i$ -th iteration. In the above equation the left hand side is the heat loss rate of a grain per unit area of grain surface. The first term on the right hand side is the rate of heat gain from the local radiation field, the second term is the rate of heat gain from the impacting gas molecules, and the last term is the rate of heat gain by the grain in question from all the other grains surrounding it. The exponential term here takes care of the fact that the radiation from the grains at location  $r$  becomes attenuated by the intervening grains in reaching the grain in question. In the preliminary analysis by *De and Arrhenius* [3], the last term in Eq.(1) was approximated as

$$\frac{1}{2} \pi \sigma a^2 \int_0^R \int_0^\pi n(r) [T_{s,(i)}(r)]^4 \sin \theta \, d\theta \, dr$$

where the assumption was that a given grain received radiation directly (without attenuation) from all the other grains within a sphere of radius  $R = [\pi a^2 n(h)]^{-1}$ , the local photon mean free path - and did not receive any radiation from the other grains. This approximation has now been removed, and Eq.(1) has been solved in its entirety. In practice, however, it was found sufficient to truncate the  $r$ -integration under the exponent at  $r = 5R$  or at the cloud boundary - whichever is nearest to the grain in question.

The method of solving Eq.(1) is first to neglect the last term and obtain a numerical solution for  $T_s$ . Since this solution refers to a case where a given grain does not receive any radiation from the other grains, it gives us the grain temperature in a region that is fully transparent for the escape of infrared radiation. This case has been discussed earlier [1]. This transparent solution constitutes  $T_{s,(1)}$  for our iterations. We next enter  $T_{s,(1)}$  in the last member of Eq.(1), and solve the equation in its entirety to obtain  $T_{s,(2)}$ . The iterations are then continued until the successive iteration values of  $T_{s,(i)}$  do not differ significantly. In this way we obtain a self-consistent solution for the disequilibrium steady state.

As a numerical illustration of the above discussion, we have chosen the much-discussed primitive solar nebula - where traditionally a complete thermal equilibrium has been assumed [4]. The nebula is visualized as a disc-shaped cloud around the sun (or protosun) - and we consider roughly the present asteroidal region (which is also often suggested to be the meteorite formation region). The grains are assumed to be metallic iron (with  $a = 0.1\mu$ ) which, with a relative abundance of  $10^{-5}$  in the nebula, is assumed to be fully condensed wherever the grain temperature is below the condensation temperature

## THERMAL DISEQUILIBRIUM IN COSMIC DUST CLOUDS

DE and ARRHENIUS

of iron. We have assumed, somewhat arbitrarily but roughly in keeping with popular nebular models [4], that the temperature  $T_k$  decreases from  $2000^\circ\text{K}$  at the midplane to  $1/e$  times this value at the surface - while the density  $N$  decreases linearly from  $10^{15} \text{ cm}^{-3}$  at the midplane to 0 at the surface. Other parameters are indicated in Figure 2. Also presented in this figure are the infrared optical depths in the nebula. Note that the condensation temperature of iron under the given conditions is around  $1400^\circ\text{K}$  [5] - so that near the midplane, solid grains cannot exist.

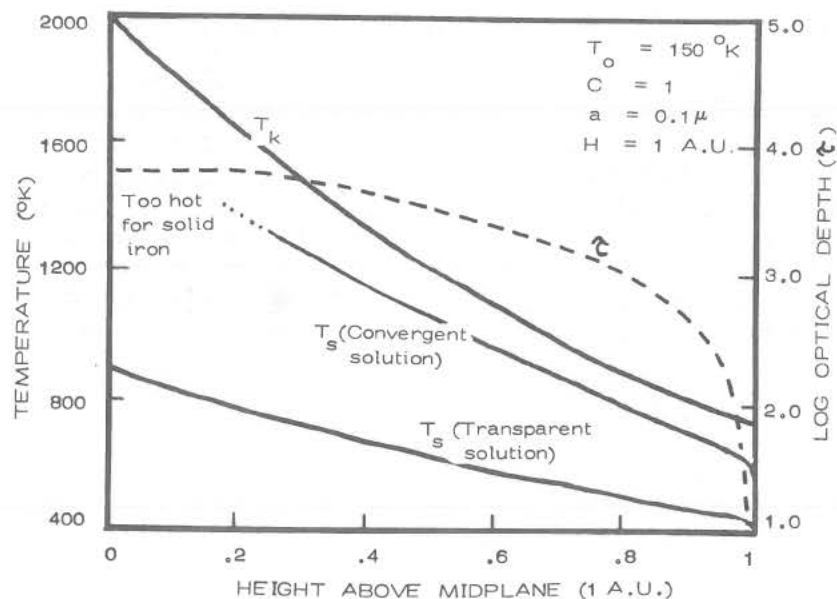


Figure 2.

While the above calculations are of a preliminary nature and several next-order refinements are called for (some of which we have discussed elsewhere [1,2]) - the general conclusion appears to be valid that even at large infrared optical depths, thermal equilibrium is not attained. When temperature-related observations in meteoritic solid phases are translated to physical conditions (temperature, pressure etc.) in the solar nebula [4], we may go completely astray. There is of course no evidence in the meteorites that indicates a temperature equilibrium in their condensation environment. Rather, analysis of thermally sensitive parameters in meteoritic metal grains appears to indicate the contrary [6].

## REFERENCES

1. B. R. De, Proc. Lunar Sci. Conf. 8th, Pergamon Press, New York, p. 79, 1977, and earlier references therein.
2. B. R. De and G. Arrhenius, Advances in Colloid and Interface Sci. (in press).
3. B. R. De and G. Arrhenius, Lunar and Planetary Sci. IX, Lunar and Planetary Institute, Houston, p. 226, 1978.
4. See e.g. review by S. S. Barshay and J. S. Lewis, Ann. Rev. Astron. Astrophys. 14, 81, 1976.
5. B. R. De, Proc. Lunar Sci. Conf. 8th, Pergamon Press, New York, p. 87, 1977.
6. G. Arrhenius and J. L. McCrumb, this volume, and earlier references therein.



CONDENSATION IN CLOUDS: EXPERIMENT AND THEORY, B. Donn, Lab. for Extraterrestrial Physics, NASA-Goddard Space Flight Center, Greenbelt, MD

An experimental and theoretical study of condensation of grains appropriate to a variety of astronomical environments is under way in the Astrochemistry Branch of the Goddard Space Flight Center. The program concentrates on the following characteristics of astronomical systems: 1. a multiple condensible species; 2. low reactant partial pressures; 3. condensation of complex, refractory oxides and silicates not present in the gas phase; 4. reactive ambient gases. The background and initial experiments are described in three papers (Donn, 1975; 1978; Day and Donn, 1978).

We are investigating an essentially neutral medium in which a low level of ionization may have significant effects on condensation. In the two papers by Donn cited above, arguments are given from which it is concluded that condensation is a kinetic process. Thermodynamics provides some general boundary conditions and cannot be used to determine details, as temperatures, composition or structure, of condensates. Experiments are under way on the dependence of nucleation on the temperature of the ambient gas for selected species. Present experimental results indicate that even at very large supersaturations nucleation is difficult at temperatures of a few hundred degrees Celsius. It is proposed that this is caused by the extreme instability of the small molecular clusters which are the initial stages of nucleation. Extension of the experiments and concomitant development of the theory are expected to lead to a kinetic theory of condensation in clouds.

B. Donn, 1975, Mem. Soc. Roy. Sci. Liege, 6th Ser. 9, 499

1978, "Protostars and Planets" ed. Tom Gehrels, Univ. of Arizona Press, (in press)

K. L. Day and B. Donn, 1978, Ap. J. 222, L45



TIME-DEPENDENT NUCLEATION THEORY AND THE FORMATION OF INTERSTELLAR GRAINS, B.T. Draine, Harvard-Smithsonian Center for Astrophysics, Cambridge Mass. 02138.

It has been known for some time that nucleation of dust grains occurs in stellar atmospheres or outflows; the products of such nucleation have been observed in circumstellar shells around cool, evolved red giants, in planetary nebulae, and in novae. Much uncertainty persists, however, regarding the nucleation process by which these grains are formed. For example, it has been difficult to account theoretically for the sizes of the particles formed. In many cases it is also not clear whether grain formation is the cause or merely a consequence of mass loss from the star. The uncertainties arise not only from incomplete understanding of stellar evolution, atmospheres, and mass-loss mechanisms, but also in part from the complexity (and controversies) of the theory of homogeneous nucleation from the vapor phase.

The theory of time-dependent nucleation in a cooling gas has been investigated both analytically and numerically in a recent paper (1) where it is assumed that "classical" nucleation theory (2) can be used to calculate the instantaneous nucleation rate. With this assumption, the character of the nucleation process is shown to depend almost entirely on just two dimensionless quantities: the ratio  $(\theta/T)$  (where  $T$  is the temperature, and  $k\theta$  is essentially the surface free energy per surface site), and a dimensionless parameter  $\eta$  which measures the number of times monomers collide with a single surface site during one supersaturation ratio  $e$ -folding time. Classical nucleation theory assumes  $\theta$  to be independent of the cluster size  $N$ , and therefore simply proportional to the bulk surface tension; this key assumption has been the subject of much theoretical (and experimental) controversy. The degree to which  $\theta$  depends on  $N$  will be discussed in light of recent experimental work; nucleation experiments with the diffusion cloud chamber (3) and with supersonic nozzles (4) suggest that  $\theta$  is essentially independent of  $N$  (at least down to  $N = 20$  or so), but recent shock tube work (5) appears to indicate a strong dependence of  $\theta$  on  $N$ . It will be concluded that the experimental evidence appears to be weighted in favor of classical nucleation theory.

The analytic treatment of time-dependent nucleation (1) will be described, and the results will be summarized. The domain within which the analytic results are applicable will be delineated, and the analytic formulae will be compared to (a) numerical integration of the nucleation-particle growth equations, and (b) laboratory measurements of nucleation in supersonic nozzles (4, 6-8). The comparisons are generally favorable, indicating that the analytic results may be confidently employed (within the domain of validity) to predict such quantities as the "critical" supercooling or supersaturation, the mean final cluster size, and the dispersion in final cluster size.

The nucleation of dust grains in stellar outflows will be briefly discussed, based on recent work by Salpeter (9-11). It will be shown how the above-described analytic results may be applied to predict the sizes of grains formed during, for example, the ejection of a planetary nebula.

#### References:

- (1) Draine, B.T., and Salpeter, E.E. 1977, J. Chem. Phys. 67, 2230.
- (2) Feder, J., Russell, K.C., Lothe, J., and Pound, G.M. 1966, Adv. Phys. 15,

## TIME-DEPENDENT NUCLEATION THEORY

Draine, B.T.

- 111.
- (3) Katz, J.L., Mirabel, P., Scoppa, C.J., and Virkler, T.L. 1976, J. Chem. Phys. 65, 382.
  - (4) Wu, B.J.C., Wegener, P.P., and Stein, G.D. 1978, J. Chem. Phys. 68, 308.
  - (5) Freund, H.J., and Bauer, S.H. 1977, J. Phys. Chem. 81, 994.
  - (6) Jaeger, H.L., Willson, E.J., Hill, P.G., and Russell, K.C. 1969, J. Chem. Phys. 51, 5380.
  - (7) Dawson, D.B., Willson, E.J., Hill, P.G., and Russell, K.C. 1969, J. Chem. Phys. 51, 5389.
  - (8) Hagena, O.F., and Obert, W. 1972, J. Chem. Phys. 56, 1793.
  - (9) Salpeter, E.E. 1974, Astrophys. J. 193, 579.
  - (10) Salpeter, E.E. 1974, Astrophys. J. 193, 585.
  - (11) Salpeter, E.E. 1977, Ann. Rev. Astron. Astrophys. 15, 267.

A NEW MODEL FOR INTERSTELLAR DUST, W.W. Duley, T.J. Miller and S. MacLean, Physics Dept., York Univ., Toronto, Canada M3J 1P3 and D.A. Williams, Mathematics Dept., UMIST, Manchester, England.

The relationship between depletion and the growth of grains in the interstellar medium is discussed. It is suggested that the depletion of elements such as Si, Mg and Fe leads to the formation of oxide grains. These grains form by the accretion of atoms and ions from the interstellar gas in a way similar to that envisioned by Donn [1]. A primitive mixture of diatomic oxides (e.g. MgO, SiO, FeO, NiO, etc.) appears to be the result of this condensation from the gas. The efficiency with which individual elements condense can be shown to depend primarily on the first ionization potential when condensation occurs on nucleation centres in diffuse clouds and in the intercloud medium. An analysis of this process [2] shows that selective depletion occurs on grains that contain coordinatively unsaturated surface  $O^{2-}$  ions ( $O^{2-}_{CUS}$ ), that is on those grains that are responsible for the  $2175\text{\AA}$  extinction feature [3]. The role of the surface in determining depletion efficiency will be discussed. This model permits detailed predictions of relative depletions to be made. Predictions of this model will be tested against measured depletions for several sets of observational data. Some important features of the model are:

- 1) P and Cl are not depleted by accretion on oxide grains in diffuse clouds as observed by Jura and York [4].
- 2) F should be depleted.
- 3) The depletion of Zn and S should be small relative to that of Ca.
- 4) Ti and Cr have large depletions but  $D(\text{Ca}) > D(\text{Cr}) \geq D(\text{Ti})$  where  $D \equiv$  depletion.
- 5) The alkali metals should be depleted less than Ca.

Further observational consequences of the mixed oxide grain model will be discussed and recent laboratory data on the infrared spectra of small particles of these materials will be compared with infrared spectra of heavily reddened sources.

We have investigated the possible role that oxide grains with chemically active surfaces may play in the formation of molecules within diffuse interstellar clouds. Our conclusions are that surface catalyzed reactions may be quite specific, leading to certain preferred product molecules and not (in general) to the wide range of products commonly assumed. Two catalytic reaction schemes that lead to the formation of HCO and  $\text{H}_2\text{O}$  on oxide grain surfaces are shown schematically in figure 1. The relevant surface sites together with an explanation of the notation used are given in figure 2 and table 1 respectively.

## Interstellar Dust

Duley, W.W. et al.

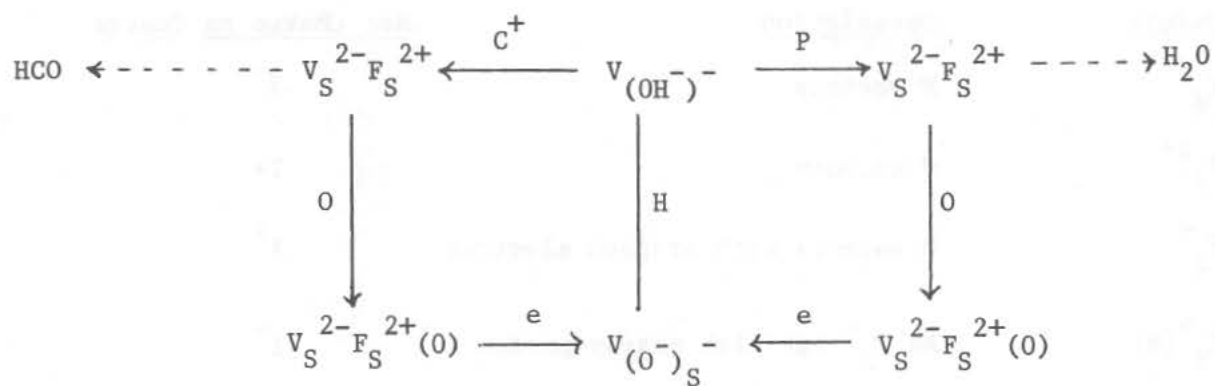


Figure 1



Figure 2

## Interstellar Dust

Duley W.W., et al.

Table 1 Surface Defects on a Diatomic Oxide

<u>Defect</u>	<u>Description</u>	<u>Net Charge on Centre</u>
$V_S^{2-}$	M vacancy	$2^-$
$F_S^{2+}$	O vacancy	$2^+$
$F_S^+$	O vacancy with trapped electron	$1^+$
$F_S^+(H)$	As $F_S^+$ but with nearby proton	$1^+$
$(O^-)_S^+$	Surface $O^-$ ion	$1^+$
$(O^-)_S$	$M^+O^-$ pair	0
$(OH^-)_S^+$	$O^{2-}H^+$ pair <u>or</u> $O^-H$ pair	$1^+$
$V_{(O^-)_S}^{2-}$	$M^+O^-$ pair adjacent to M vacancy	$2^-$
$V_{(O^-)_S}^-$	$O^-$ adjacent to M vacancy	$1^-$
$V_{(OH^-)_S}^-$	As $(OH^-)_S^+$ but with adjacent M vacancy	$1^-$

References

1. Donn, B., Mem. Soc. Roy. Sci. Liège, 6<sup>e</sup> série, 10, 499 (1976).
2. Duley, W.W. and Millar, T.J., Ap. J., 220, 124 (1978).
3. Duley, W.W., Astrophys. Sp. Sci., 45, 253 (1976).
4. Jura, M and York, D.G., Ap. J., 219, 861 (1978).

ASSOCIATION REACTIONS; E. Herbst, Dept. of Chem., College of William and Mary, Williamsburg, VA 23185.

Association reactions are chemical condensation processes in which two smaller species, A and B, unite to form a larger species AB:



There are two principal mechanisms by which association reactions can occur; these mechanisms are designated as three-body association and radiative association. In the three-body process, molecules A and B collide to form an unstable "collision complex"  $AB^*$  which can be collisionally stabilized by a third species, designated M:



A variant of this mechanism can occur if species M is itself chemically reactive with species A or B. Then, the following series of processes is possible:



Processes (2) and (3) comprise the "energy transfer" route and processes (4) and (5) the "chaperone" route to three-body association.<sup>1</sup> Species M need not be a single molecule but can refer to a large cluster of molecules or even a dust particle.

The other association process, radiative association, is important only at very low pressures (such as pertain in interstellar clouds) and occurs via the mechanism





## ASSOCIATION REACTIONS

Herbst, E.

that is, stabilization of the collision complex  $AB^*$  occurs via the emission of photons.

Association reactions play an important role in atmospheric<sup>2</sup> and interstellar<sup>3</sup> chemistry. Three-body association processes have been studied extensively in the laboratory for the situation in which one of the associating species is an ion.<sup>4</sup> These ion-molecule reactions are of unusual chemical interest because their rate coefficients are inversely proportional to the temperature raised to powers sometimes as high as 4 or greater.<sup>3</sup> We have recently developed a simple theory to explain both the temperature dependence and absolute value of the rate coefficient for assorted ion-molecule association reactions, both three-body and radiative. Unlike earlier approximate theories,<sup>5</sup> our new work incorporates the principle of detailed balancing,<sup>6</sup> which relates the formation and destruction rates of the intermediate collision complex. Comparison of the theory with some experiments will be provided. It is hoped that the theory can be utilized to estimate the rates of a wide variety of three-body and radiative associations and thereby increase our understanding of these important condensation processes.

References

1. R. E. Weston, Jr. and H. A. Schwarz, Chemical Kinetics (Prentice-Hall, Englewood Cliffs, N.J., 1972).
2. See, for example, F. C. Fehsenfeld and E. E. Ferguson, Planet. Space Sci. 20, 295 (1972).
3. D. Smith and N. G. Adams, Astrophys. Jour. 220, L87 (1978).
4. See Reference 3 or F. C. Fehsenfeld, D. B. Dunkin, and E. E. Ferguson, Astrophys. Jour. 188, 43 (1974).
5. See, for example, E. Herbst, Astrophys. Jour. 205, 94 (1976) or M. Meot-ner and F. H. Field, Origins of Life 6, 377 (1975).
6. For a similar although less useable treatment of this idea, see D. R. Bates, Proc. Roy. Soc. London 360A, 1 (1978).

ORGANIC DUST SYNTHESIZED IN REDUCING ENVIRONMENTS BY  
ULTRAVIOLET RADIATION OR ELECTRIC DISCHARGE

B.N. Khare and Carl Sagan  
Laboratory for Planetary Studies  
Cornell University  
Ithaca, New York 14853

A dark reddish-brown high molecular weight polymer is produced by long wavelength ultraviolet irradiation of abundant gases present in reducing atmospheres,  $\text{CH}_4$ ,  $\text{C}_2\text{H}_6$ ,  $\text{NH}_3$ ,  $\text{H}_2\text{O}$ , and  $\text{H}_2\text{S}$ . The photodissociation of  $\text{H}_2\text{S}$  yields a hydrogen atom which is superthermal by several electron volts and which drives subsequent chain reactions.<sup>1,2</sup> In a typical experiment (Figure 1), the inner walls of the reaction vessel are characteristically coated, after a few hours of irradiation, with a brownish solid.

This solid material shows some spectrometric similarity to the brown clouds observed on Jupiter, Saturn, and Titan.<sup>3</sup> After a typical photolysis experiment the brown solid after extraction with benzene is 84 percent sulfur, largely  $\text{S}_8$ . The remaining 16 percent was pyrolyzed and then examined by gas chromatography -- mass spectrometry. Pyrolysis<sup>4</sup> at  $450^\circ\text{C}$  yields the rich array of compounds shown in Table 1.

In another experiment (Figure 2), similar dark brown polymeric material is produced by electric discharge through a mixture of  $\text{CH}_4$ ,  $\text{NH}_3$ , and  $\text{H}_2\text{O}$  (vapor) which on pyrolysis at  $600^\circ\text{C}$  yields a similar list of compounds.

The dust produced under conditions similar to those described in these two examples may be relevant to the observed ultraviolet, visible and infrared spectroscopic characteristics of planetary atmospheres and the interstellar medium.

The synthesized polymers are stable to about  $1000^\circ\text{K}$ . Another solid material that we consider important is hexamethylenetetramine (HMTA) that is obtained stoichiometrically from ammonia and formaldehyde. HMTA on heating produces largely HCN. From the infrared spectra of this polymer after heating to  $923^\circ\text{K}$ , we propose that the tradition of attributing the 9 to  $13\ \mu\text{m}$  interstellar features to silicate dust or pure graphite should be reexamined. Our infrared study of the polymers produced both by ultraviolet light and electric discharge, their stability at high temperatures, Douglas' proposal<sup>5</sup> of explaining the diffuse interstellar line at  $4428\ \text{\AA}$  and the continuum at  $2200\ \text{\AA}$  by polyatomic molecules containing carbon as  $\text{C}_n$  ( $5 \leq n \leq 15$ ), and other arguments,<sup>6</sup> suggest organic polymers as major constituents of interstellar dust.

Some of the physical and chemical properties of the dust produced in our laboratory will be presented. Brown solid flakes produced by electric discharge through a mixture of  $\text{CH}_4$ ,  $\text{NH}_3$ , and  $\text{H}_2\text{O}$  (vapor) will be available for visual inspection.

## ORGANIC DUST SYNTHESIZED IN REDUCING ENVIRONMENTS

Khare, B.N., Sagan, C.

References

1. C. Sagan and B.N. Khare, Science 173, 417 (1971); B.N. Khare and C. Sagan, Nature (London) 232, 577 (1971).
2. C. Sagan and B.N. Khare, Astrophys. J. 168, 563 (1971).
3. B.N. Khare and Carl Sagan, Icarus 20, 311 (1973).
4. B.N. Khare, Carl Sagan, Eric L. Bandurski and Bartholomew Nagy, Science 199, 1199 (1978).
5. A.E. Douglas, Nature 269, 130 (1977).
6. C. Sagan, Nature 238, 77 (1972).

## ORGANIC DUST SYNTHESIZED IN REDUCING ENVIRONMENTS

Khare, B.N., Sagan, C.

Table 1. Polymer components from the ultraviolet synthesis experiments (the initial mixture consisted of  $\text{CH}_4$ ,  $\text{C}_2\text{H}_6$ ,  $\text{NH}_3$ ,  $\text{H}_2\text{S}$ , and  $\text{H}_2\text{O}$ ). From Ref. (4).

Compounds identified	Relative abundance*	Molecular weight	Compounds identified	Relative abundance*	Molecular weight
Hydrogen sulfide	M	34	2-Methylthiophene	M	98
Carbon dioxide	M	44	3-Methylthiophene	M	98
Carbonyl sulfide	M	60	Ethylthiophenes	M	112
Hydrogen cyanide	M	27	Dimethylthiophenes	M	112
Ammonia	M	17	$\text{C}_3$ -alkylthiophenes	m	126
Carbon disulfide	M	76	$\text{C}_4$ -alkylthiophenes	m	140
Ethane	M	30	Methylmercaptan	M	48
Propane	M	44	Ethylmercaptan	M	62
Butane	m	58	Propylmercaptan	M	76
Ethene	M	28	$\text{CH}_3-\text{S}-\text{S}-\text{CH}_3$	M	94
Propene	M	42	$\text{C}_3$ -alkyl(-S-S-)†	M	108
Butene	M	56	$\text{C}_4$ -alkyl(-S-S-)†	M	122
Pentene	M	70	$\text{C}_5$ -alkyl(-S-S-) s†	M	136
Hexene	m	84	$\text{C}_6$ -alkyl(-S-S-)†	M	150
Heptenes	m	98	$\text{CH}_3-\text{N}=\text{C}=\text{S}$ (methyl isothiocyanate)	M	73
Butadiene	M	54	$\text{CH}_3\text{CH}_2-\text{N}=\text{C}=\text{S}$	M	87
Methyl cyclopentene	t	82	$\text{C}_3$ -alkyl-N=C=S s	M	101
Hexadiene	t	82	$\text{C}_4$ -alkyl-N=C=S	M	115
Hexyne	t	82	$\text{C}_5$ -alkyl-N=C=S	m	129
Butadiyne	t	50	$\text{CH}_2=\text{CHCH}_2-\text{N}=\text{C}=\text{S}$	m	99
Benzene	M	78	$\text{CH}_3\text{CN}$	M	41
Toluene	M	92	$\text{CH}_2=\text{CH}-\text{CN}$	M	53
Xylene	m	106	$\text{CH}_3-\text{CH}=\text{CH}-\text{CN}$	m	67
$\text{C}_3$ -alkylbenzene	m	120	Benzonitrile	m	103
Styrene	m	104			
Thiophene	M	84			

\*M, major component; m, minor component; t, tentative identification. †These compounds are alkyl disulfides (dithioalkanes);  $\text{C}_4$ -alkyl(-S-S-), for example, is either  $\text{CH}_3\text{CH}_2\text{CH}_2-\text{S}-\text{S}-\text{CH}_3$  or  $\text{CH}_3\text{CH}_2-\text{S}-\text{S}-\text{CH}_2\text{CH}_3$ . A lowercase s after a compound indicates that two or more isomers are present.

## ORGANIC DUST SYNTHESIZED IN REDUCING ENVIRONMENTS

Khare, B.N., Sagan, C.

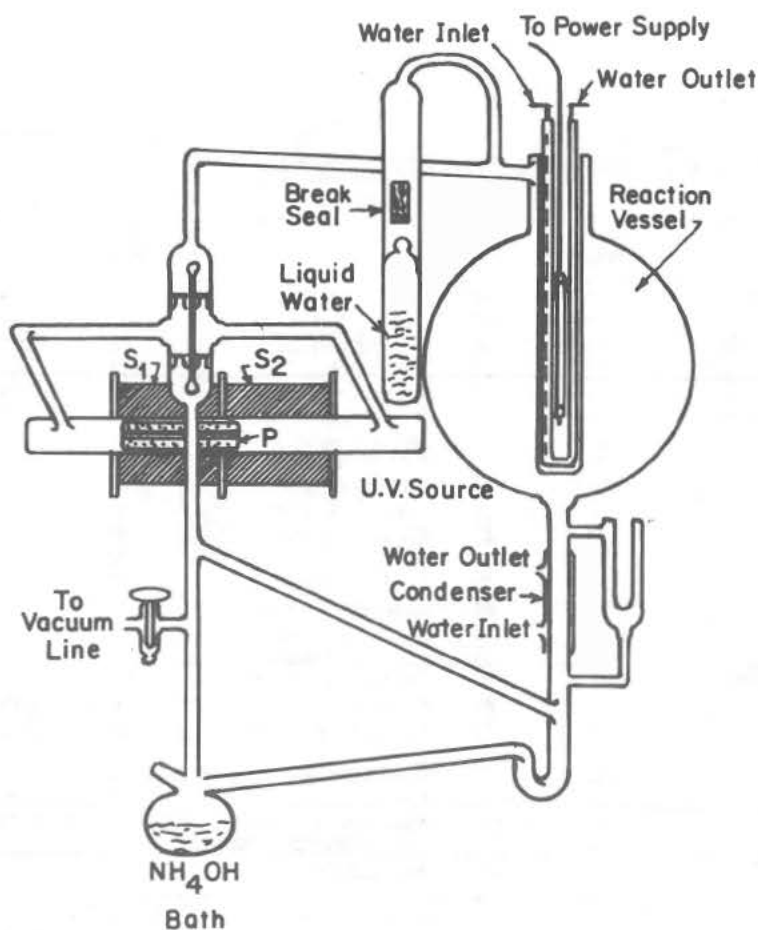


Figure 1. Experimental apparatus for photochemistry in reducing atmospheres. The Hg-discharge lamp irradiates initial reactants in the reaction vessel, which are circulated through the simulated ammonium hydroxide clouds (lower left) by the Watson pump (upper left).

## ORGANIC DUST SYNTHESIZED IN REDUCING ENVIRONMENTS.

Khare, B.N., Sagan, C.

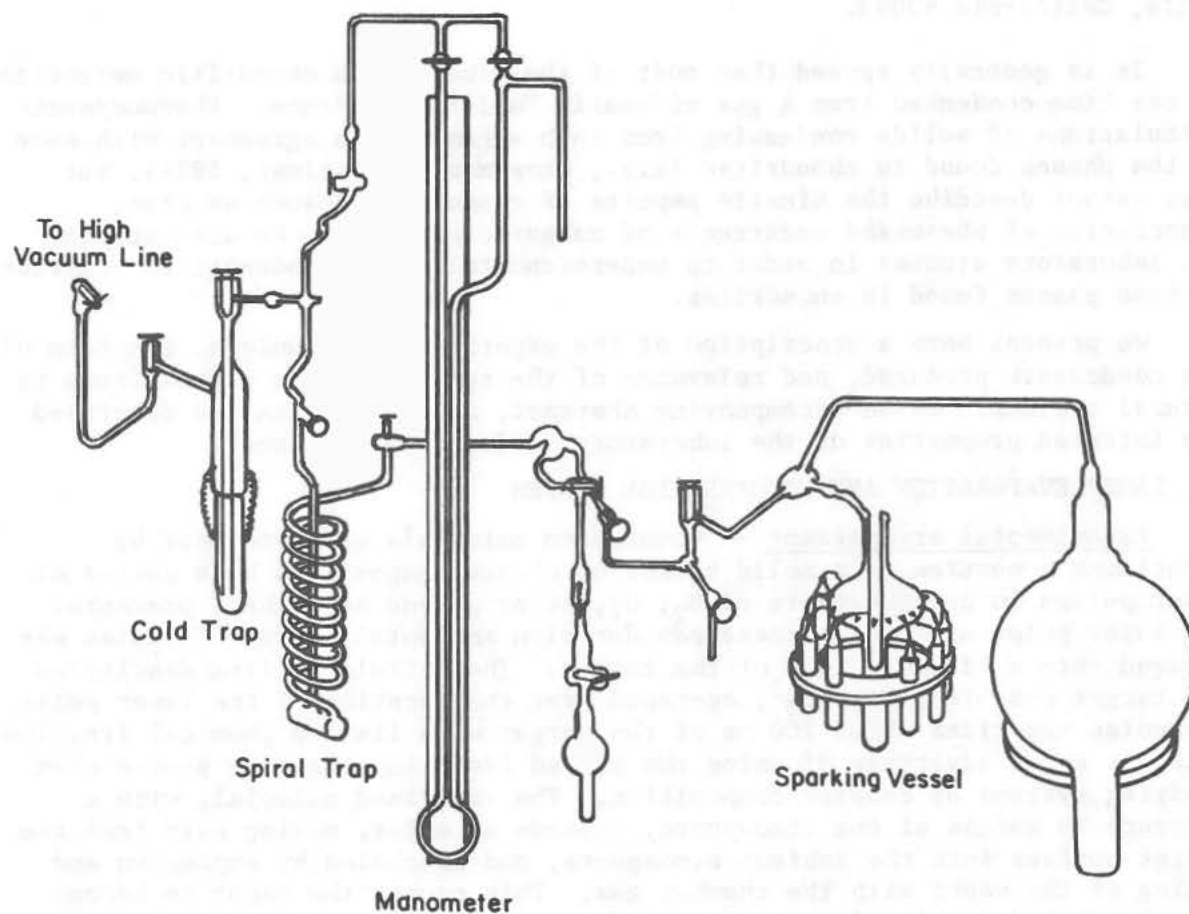


Figure 2. Experimental apparatus for electrical discharge experiments in reducing atmospheres.



# LABORATORY CONDENSATION OF CHONDRITIC MINERALS;

B. K. Kothari and J. R. Stephens, University of California, San Diego, La Jolla, California 92093.

It is generally agreed that most of the minerals in chondritic meteorites at one time condensed from a gas of nearly "solar" abundance. Thermodynamic calculations of solids condensing from such a gas are in agreement with some of the phases found in chondrites (e.g., Grossman and Larimer, 1974), but they cannot describe the kinetic aspects of condensation such as size, association of phases and occurrence of metastable phases. We are carrying out laboratory studies in order to understand fully the condensation behavior of some phases found in chondrites.

We present here a description of the experimental technique, the form of the condensate produced, and relevance of the results to the phases found in natural systems. In an accompanying abstract, J. R. Stephens has described the infrared properties of the laboratory produced condensates.

## I. LASER EVAPORATION AND CONDENSATION SYSTEM

Experimental arrangement -- Condensate materials were produced by vaporizing a portion of a solid target of chosen composition by a series of laser pulses in an atmosphere of  $H_2$ ,  $O_2$ , or Ar at one atmosphere pressure. The laser pulse of  $\sim 500$  microseconds duration and total energy  $\sim 5$  joules was focused onto a  $\sim 1$  (mm)<sup>2</sup> area of the target. The calculated flux density on the target was  $\sim 10^6$  watts/cm<sup>2</sup>, averaged over the duration of the laser pulse. The pulse vaporizes about 200  $\mu g$  of the target with limited chemical fractionation, a major advantage of using the pulsed laser as a heating source when studying systems of complex composition. The vaporized material, with a pressure in excess of one atmosphere, expands as a jet, moving away from the target surface into the ambient atmosphere, and is cooled by expansion and mixing of the vapor with the chamber gas. This causes the vapor to become supersaturated within microseconds, and to nucleate into  $\sim 1$  nm droplets.

Grain growth occurs predominantly by droplet collisions due to thermal motions, since the number density of the original condensate droplets is high ( $> 10^{10}$  grains/cm<sup>3</sup>). The grains solidify within milliseconds, and coagulate to form chains. The resulting condensate smoke consists, in most cases, of tangled strings made up of grains which have a median diameter of 20-30 nm. The condensate is analyzed by Scanning and Transmission Electron Microscopy.

Some of the important features of the condensation technique are: (1) Condensation takes place in a time scale less than milliseconds without any interaction with the cell wall from a gas jet above 1 atm pressure. Except for substances with triple points greater than 1 atm (e.g., C and SiC), all of the systems studied condense as a liquid droplet and solidify upon cooling. (2) Irrespective of the chemistry of the target and ambient gas, the condensate occurs as chains of 10-40 nm diameter grains. (3) The condensate collected from experiments performed in reactive gas atmospheres exhibit chemistry which reflects both the composition of the target and the

## LABORATORY CONDENSATION OF CHONDRITIC MINERALS

B. K. Kothari and J. R. Stephens

ambient gas. For example, Fe vaporized in  $O_2$  and in  $H_2S$ , yield condensates of  $Fe_2O_3$  and FeS respectively. This allows control to be exercised on the chemistry of the condensate by selecting the proper target-ambient gas combinations. (4) While silicates, calcium carbonate and carbon are found to condense as amorphous grains, the other condensates studied are collected as crystalline grains. In some condensates --  $\gamma Al_2O_3$ , fcc Mo, Mo-V and Co--metastable phases were identified.

Condensation of silicates -- To study the condensation of silicates of approximately olivine and pyroxene composition, targets were prepared by mixing various combinations of  $SiO$ ,  $MgO$ ,  $Fe_2O_3$  and Fe powders and vaporized in gas mixtures of Ar,  $O_2$ ,  $H_2$  and  $H_2O$ . The wide variety of chemical conditions allowed the successive oxidation of the Mg, Si and Fe in silicate-like minerals to be studied. The phases found under increasingly oxygen-rich conditions indicates that the grains are collected with the various components in internal equilibrium. The results are discussed in detail in Stephens and Kothari (1978a).

Condensation of immiscible phases -- To model the condensation of multi-phase gas, the model systems, Au- $Al_2O_3$ , Cu-C, Au-olivine, in which the phases are immiscible in both liquid and solid phases were vaporized. The condensate consists of 5-50 nm particles of individual phases intimately mixed together in chains. The meteorites -- Allende, Orgueil and Abee -- were vaporized in  $H_2$ , Ar and  $O_2$ . In all the cases the condensate contains a glass phase and a crystalline phase depending upon the meteorite and the ambient gas. The results will be discussed.

## II. RELEVANCE OF LABORATORY EXPERIMENTS TO CONDENSATION IN NATURAL SYSTEMS

While our experiments do provide data on the condensation of cosmically abundant elements at high pressures, the results must be extrapolated to lower pressures characteristic of natural condensation processes. Particularly, the occurrence of condensate as chains of submicron particles, condensation of metastable and immiscible phases are examined to see if such structures are formed at lower pressures also. The laboratory condensates are then compared with the natural systems to derive information concerning their formation conditions.

Natural solids can be divided into two categories. Cosmic dust may have simple condensation histories but can only be studied observationally and is thus not well characterized (e.g., Huffman, 1977). In contrast, meteorites and interplanetary particles of Brownlee, *et al*, are amenable to detailed laboratory studies. However, meteorite samples occur as compact bodies and the geochemical history of many of the constituent phases is hotly debated at present.

Similarities of laboratory produced grains with the cosmic dust are treated in Stephens and Kothari (1978b).

Submicron nature of the condensate -- The condensates produced by many vapor condensation processes occur as chains of submicron grains and are well studied in the engineering literature (e.g., Hidy and Brock, 1970). Vaporization of solids in an inert gas atmosphere at a pressure of about  $10^{-3}$  atm also yield condensates consisting of chains of submicron particles (e.g., Granquist and Buhrman, 1976). The grain diameters of our condensate systems show an approximately log-normal distribution which is consistent with the growth of grains by coagulation due to high supersaturation of the gas

## LABORATORY CONDENSATION OF CHONDRITIC MINERALS

B. K. Kothari and J. R. Stephens

and hence large particle densities.

If the condensation in natural system occur by low supersaturation, the particle density will be low & particles will grow mainly by molecular growth. Kothari (1978) has calculated the minimum time needed to grow particles of various sizes in both high and low supersaturation cases for pressures characteristic of a solar nebula environment.

The submicron matrix minerals of unequilibrated chondrites have been found to follow a log-normal distribution (Ashworth, 1977). The grain growth may then have taken place predominantly by coagulation. If so, the condensation time may be near the time defined by the high supersaturation. Implications for the condensation of solar system matter will be discussed.

Arnold (1977) has discussed the agglomeration of grains under conditions postulated for a solar nebula.

Metastable phases -- Metastable glasses and crystal phases in our experiments are believed to result from the fast cooling rates ( $10^5$ - $7 \times 10^6$  °K/sec at  $1500^\circ$  K) of the condensate particles (Stephens and Kothari, 1978c). Two factors should favor the formation of metastable phases in natural solids. The condensation temperatures are lower than those of the laboratory experiments due to lower gas pressures of the natural systems. The grain temperature, in addition, may be lower than the gas temperature due to efficient radiative cooling of the grains (Arrhenius and De, 1973). However, the grains in the natural systems are not cooled substantially by gas collisions which is the most efficient cooling mechanism for our grains, and must cool much more slowly. For example, by one model (Fix, 1971) the cooling rate of particles in stellar atmosphere is found to be  $\sim 10^{-3}$ - $10^{-4}$  °K/sec.

The direct evidence for the existence of "primordial" metastable phases in natural system is scanty. Disordered submicron silicate grains constitute a major portion of interplanetary particles of Brownlee, *et al* (1978). Laboratory spectra of glassy olivine condensates give a good match to the "10  $\mu$ m" astronomical feature, as do layer lattice silicates. Further astronomical and laboratory studies are needed to determine the conditions which are necessary for the formation of metastable silicate feature (J. R. Stephens, this volume).

Multiphase structures -- In our modal experiments, condensates of immiscible phases occur as 5-50 nm sized grains of pure phases intimately mixed together. The size and intimate association of the phases is due to high number density of grains which results in high collision rates. Irrespective of the pressure of the system if the grains of immiscible phases form at the same time and grow by coagulation, structures similar to our laboratory condensates are expected. However, if the nucleation and growth of only one phase takes place at a time then agglomerates consisting of only that phase will be found. In this way, the association of phases in meteorites and other natural systems may provide clues to the nature of the condensation process.

Analysis of minerals in chondrites and interplanetary particles of Brownlee, *et al* point towards different conditions during condensation of these objects (Kothari, 1978). Analyses of areas as small as  $10 (\mu\text{m})^2$  of submicron matrix of carbonaceous chondrites and interplanetary particles show a cosmic abundance of elements within a factor of two. This implies that the elements which comprise these samples condensed without significant fractionation. In contrast, some fine grained inclusions in Allende meteorite

## LABORATORY CONDENSATION OF CHONDRITIC MINERALS

B. K. Kothari and J. R. Stephens

contain high proportions of vapor condensed refractory phases, rich in elements such as Ca, Mg, and Ti (Boynton, 1975). The minerals comprising these inclusions must have formed in a region or time separate from the rest of the meteorite matrix.

CONCLUSIONS

1. Laser evaporation technique is capable of producing gas phase of almost any composition for condensation studies.
2. The technique has been used to study condensation of some minerals found in meteorites. The results of these experiments provide a basis for comparison with the natural systems.
3. The condensate from these experiments can be used as an analogue for studying spectral properties of cosmic dust.

REFERENCES

- Arnold, J. R. (1977) Comets, Asteroids and Meteorites, A. H. Delsemme Editor, The University of Toledo, p. 519.
- Arrhenius, G. and De, B. R. (1973), Meteoritics **8**, p. 297.
- Ashworth, J. R. (1977) Earth Planet. Sci. Lett. **35**, p. 25.
- Boynton, W. V. (1975) Geochim. Cosmochem. Acta **39**, p. 569.
- Brownlee, D. E., Tomandl, D. A., and Olszewski, E. (1977) Proc. 8th Lunar Sci. Conf., Geochim. Cosmochem. Acta **I**, p. 149.
- Fix, J. D. (1971) Kitt. Peak Contribution No. 554.
- Granquist, C. G. and Buhrman, R. A. (1976) J. Applied Phys. **47**, p. 2200.
- Grossman, L., and Larimer, J. W. (1974) Rev. Geophys. Space Phys. **12**, p. 71.
- Hidy, G. M. and Brock, J. R. (1970) The Dynamics of Aerocolloidal Systems. Pergamon Press, Chapter 9.
- Kothari, B. K. (1978) Lunar Sci. **IX** (abstract), p. 558.
- Stephens, J. R. and Kothari, B. K. (1978a) Lunar Sci. **IX** (abstract), p. 1107.
- Stephens, J. R. and Kothari, B. K. (1978b) The Moon and the Planets (in press).
- Stephens, J. R. and Kothari, B. K. (1978c) in preparation.



NUCLEATION, GROWTH AND TRANSFORMATION OF AMORPHOUS AND CRYSTALLINE  
SOLIDS CONDENSING FROM THE GAS PHASE

E. Krikorian and R. J. Sneed, Applied Research Laboratory, General  
Dynamics, Pomona Division, Pomona, CA 91766

The topic of this paper is the condensation of solids, traced from the formation of the initial critical or stable nuclei through the growth into coalesced matter. The emphasis is on: a) the definition of substrate and gas phase parameters governing the kinetics of the process, b) the conditions leading the formation of either glassy (amorphous) or crystalline solid phases, and c) the conditions causing the transition of the condensed phase from an amorphous to a crystalline state.

Impetus for this work were early findings by the authors<sup>1</sup> on the systematic growth kinetics and structural controllability of thin films. The process independent control parameters established in the referenced work were later found applicable to a large number of material systems. To gain further insight into the controlling mechanisms, a study was undertaken to explore the early nucleation processes as a function of the observed thin film control parameters and to correlate the resulting nucleation and film growth characteristics. Results of the later work constitute the content of this paper.

The material presented is based on carefully controlled experiments and a semi-empirical analysis of the experimental results. The experimental work included real time electron microscopy of the nucleation and growth process, i.e. observations of in-situ condensation.

To establish a comprehensive description of the nucleation and growth processes, a diversified and extensive range of experimental parameters and conditions were explored. Amorphous, polycrystalline as well as single crystal substrates were used. Substrate temperature was a controlled variable as was the gas phase particle flux impinging on the substrate surface. The kinetic energy of the gas phase particles was used as another experimental parameter with energies ranging from thermal levels (ambient) to values of several hundred electron volts. In all cases, the environmental backgrounds were high to ultra-high vacuum conditions. The gas phase to be condensed was generated by vacuum evaporation or sputtering, the former yielding the low kinetic energy phase the latter the high energy counterpart. Specifically, sputtering with ion beams having energies ranging from 1 KV to 30 KV led to the highest gas phase particle energies referred to above.

1. E. Krikorian and R. J. Sneed; J.A.P. 37, 10 3665 (1966).



## NUCLEATION, GROWTH AND TRANSFORMATION

Krikorian, Sneed

In the presentation, the very initial nucleation stages of the condensed phase formation are illustrated for two monatomic substances - germanium and tantalum. However, the information on post-nucleation growth kinetics and structural control parameters (amorphous versus crystalline) is shown for a large variety of materials including dielectric, semiconductive and metallic substances as well as monatomic and compound deposits. The latter include compounds reactively formed on the substrate surface in the presence of a partial pressure of reactive gas.

As the experimental results presented will show, all substrate, gas phase and environmental variables listed have distinct and systematic effects on the condensation history and on the structural characteristics of the condensed phase. Figure 1 gives an example of the substrate temperature effect on the generation of nucleation clusters as well as the saturation density of such clusters. Negative slopes correspond to coalescence of clusters as time proceeds.

While the presentation will cover extensive illustrations of experimental results and their analytical interpretation, the following is a sampling of the results and conclusions to be presented.

In all cases studied, the initial condensation process can be quite well described by basic nucleation theories, modified for such factors as particle kinetic energy, as long as the conditions results in crystalline nucleation. In these cases the data yield well defined critical nuclei sizes ( $n^* + 1$ ) for each material system as well as the energies of adsorption, surface diffusion etc. that describe the nucleation and growth kinetics. Figure 2 is an example of the excellent behavior of the experimental observations - showing in this case a consistent critical nucleus size of  $n^* + 1 = 2$  for germanium on two different substrates and at different temperatures. In this figure, the growth rate,  $R_g$  is considered proportional to the particle impingement flux. The validity of such results was facilitated by direct measurement of nucleation clusters from sizes smaller than 30Å, that is clusters containing as few as ten atoms.

Nucleation and growth starting with amorphous condensation did not conform to basic nucleation theories and had to be empirically described. The most revealing finding in this case was that amorphous condensation clearly occurs at substrate temperatures and particle flux densities insufficient to support the formation of critically sized or stable nuclei. Also the growth kinetics of initially amorphous condensates differ drastically from that of initially crystalline condensates. Figure 3

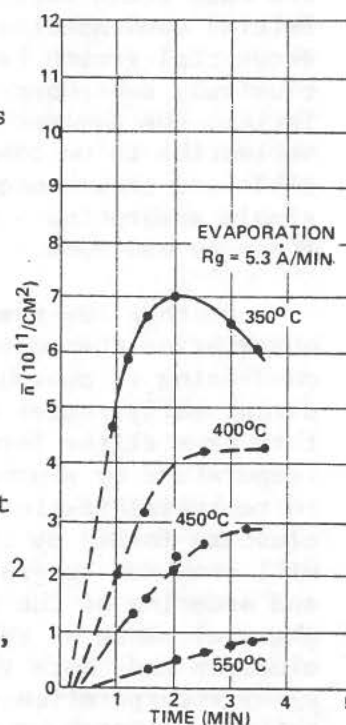


Figure 1 Temperature Dependence of Nucleation History - Ge on Carbon

## NUCLEATION, GROWTH AND TRANSFORMATION

Krikorian, Sneed

gives an example of the cluster formation rate as a function of inverse temperature for condensation of low energy germanium on two different substrates. As noted the effective activation energy ( $Q_{\text{eff}} \sim [(n^* + 1) Q_{\text{ad}} + E n^* - Q_{\text{d}}]$ ) changes from positive to negative values, and absolute values differ significantly between purely crystalline nucleation and crystalline nucleation evolving from amorphous condensation. In the case where both the very initial condensation and the sequential growth has exclusively amorphous characteristics, the concept of nucleation is no longer applicable and growth occurs by simple adsorption - typically in a one by one mode.

Another key result was the observation that material, initially condensing in amorphous form will, during early stages of growth change into crystalline form at a critical temperature by a process analogous to recrystallization. Crystalline clusters formed by this process will continue to grow a) by adsorption and ordering of the impinging gas phase elements on the crystalline clusters and, more interestingly, b) by incorporation and crystallization of amorphous material condensed in the vicinity of the crystalline clusters. The second mechanism is effective over surprisingly large distances. Figure 4 is a schematic representation of this phenomenon. The presentation includes actual electron micrographic and diffraction patterns to substantiate this schematical representation.

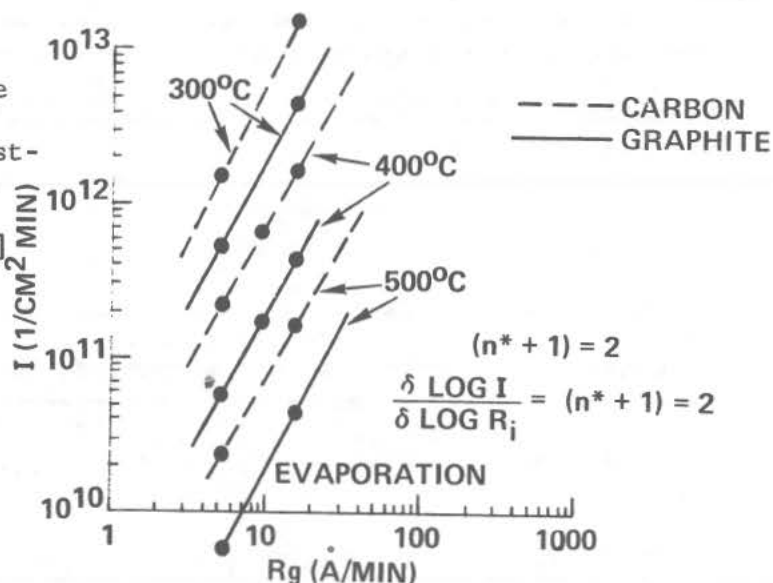


Figure 2 Nucleation Cluster Formation Rate vs. Gas Particle Impingement Rate - Evaporated Ge

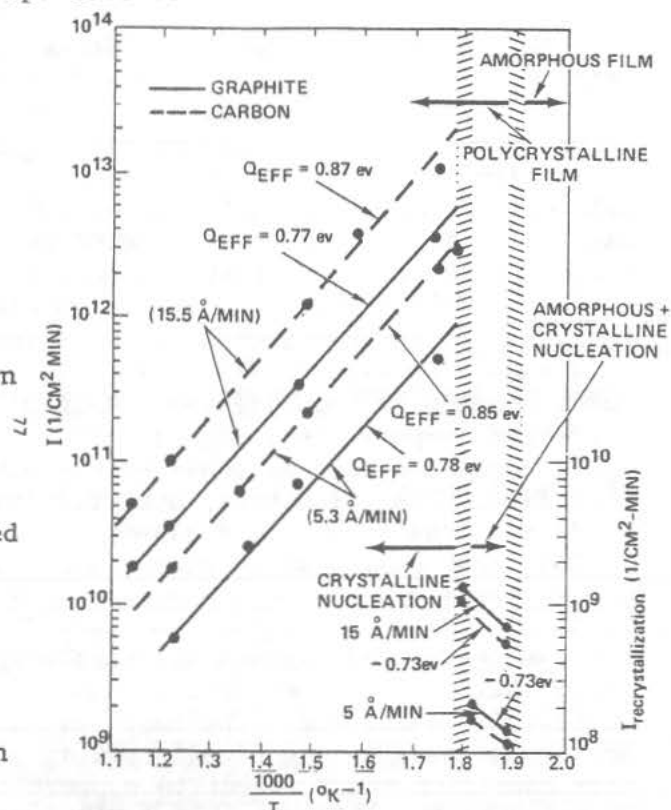


Figure 3 Temperature Dependence of Nucleation Rate - Evaporated Ge

## NUCLEATION, GROWTH AND TRANSFORMATION

Krikorian, Sneed

Shown in Figure 4 are, as a function of substrate temperature, typical condensation histories from initial nucleation to final, coalesced film formation. Arrows on D and n symbols show the time and temperature dependences of the cluster dimensions and the nucleation cluster density, respectively. Noteworthy is the reversal in the temperature dependency on n between the two condensation modes.

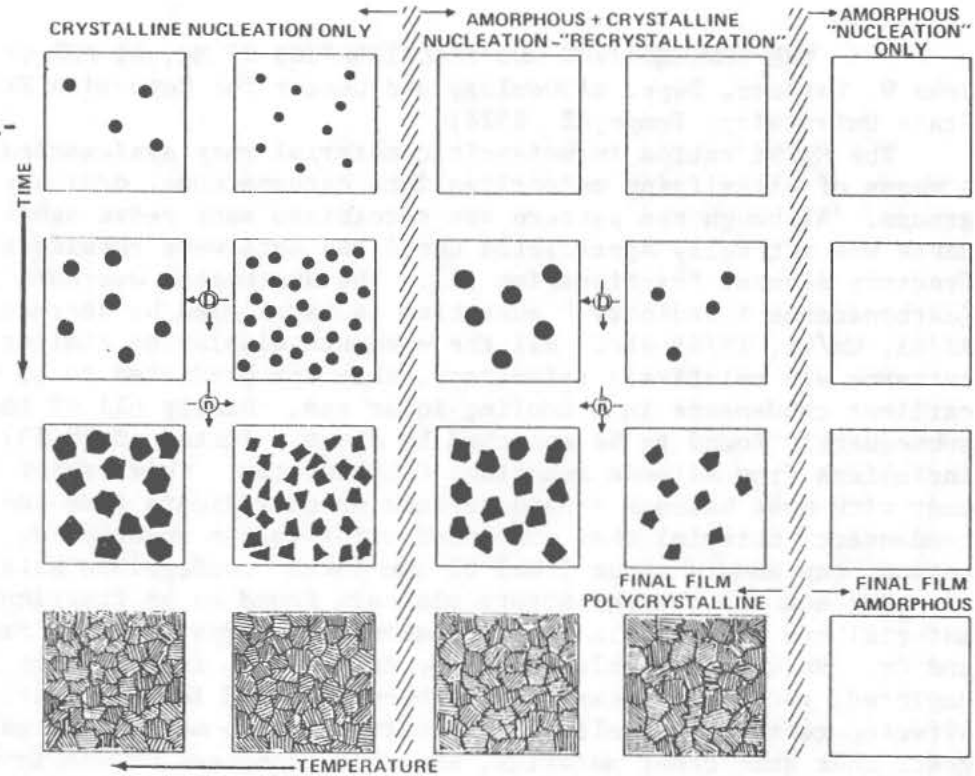


Figure 4 Schematic Nucleation and Cluster Growth Behavior on Non-single Crystal Substrates (e.g. carbon and graphite)

In summary, the research leading to the results presented gave a fairly consistent description of the basic processes. Particularly rewarding was the generality in the observed trends of condensed phase formation behavior for all materials studied.

# THE CONDENSATION AND FRACTIONATION OF Mg, Si AND Cr

John W. Larimer, Dept. of Geology and Center for Meteorite Studies, Arizona State University, Tempe, AZ 85281

The Mg/Si ratios in meteoritic material vary systematically and serve as a means of classifying meteorites into carbonaceous, ordinary or enstatite groups. Although the pattern was recognized many years ago [1], its significance was not fully appreciated until the data were considered in terms of refractory element fractionation [2]. The systematic decrease in Mg/Si ratio (carbonaceous > ordinary > enstatite) is paralleled by decreases in the ratios Al/Si, Ca/Si, Ti/Si etc. All the elements displaying similar fractionation patterns are relatively refractory; they are predicted to be enriched in the earliest condensate in a cooling solar gas. Nearly all of the elements were subsequently found to be enriched by about a factor of 20 [3] in the peculiar inclusions from Allende and other C-chondrites. This factor of 20 is consistent with mass balance considerations which indicate that the mass of the early condensate, material that condensed prior to the onset of Mg, Si and Fe condensation, represents about 5 Wt% of the total condensible material.

But not all the refractory elements found to be fractionated in meteoritic material are enriched in the inclusions. The most notable exceptions are Mg and Cr. Neither is enriched in the inclusions; in fact they are both slightly depleted, yet both appear to have been involved in the fractionation which affected refractory element concentrations in meteoritic material. This suggests that some other material, enriched in Mg and Cr, was involved in the fractionation process. The most likely candidate is olivine ( $\text{Mg}_2\text{SiO}_4$ ), the first major Mg-Si bearing condensate [2]. The fractionation of olivine with its Mg/Si ratio of 2 along with all the other, even more refractory elements, qualitatively accounts for the patterns observed in chondritic meteorites.

To see if it is quantitatively possible the fractionation patterns have been re-examined in some detail. Element ratios (e.g. Si/Al vs. Mg/Al) were plotted to determine the fractionation trends. In all cases the fractionation line drawn through the C and H, L and LL data (both of which form tight clusters) also passes through the E - chondrite data. There are several implications: 1) the process apparently involved material of a unique composition falling somewhere along the fractionation line and 2) as noted previously [2] the extent of the fractionation was virtually identical for all ordinary chondrites but varied somewhat for enstatite chondrites.

The composition of the refractory component that was fractionated can be estimated from the point of intersection between the line depicting the variation in composition of the condensate and the fractionation line. On the assumption that all of the Al is condensed at the time of fractionation, the Mg/Al and Si/Al ratios in the condensate are 10.3 and 6.65. This indicates that about .87 of the Mg and 0.57 of the Si had condensed. In a cosmic gas, a condensate of this composition occurs just prior to the point at which  $\text{MgSiO}_3$  begins to form. The most straightforward interpretation is that an early condensate of this composition was partially removed from the source region of the ordinary and enstatite chondrites.

Since carbonaceous chondrites such as Allende do not appear to have lost any of this component, and may even be slightly enriched in it, an attempt

## The Condensation and Fractionation of Mg, Si and Cr

John W. Larimer

was made to search for the appropriate olivine component. One clue was the observation that Cr is depleted to about the same extent as Mg. The behavior of Cr in a cosmic gas is unclear. Some metal grains in C-chondrites are slightly enriched in Cr [4]. But if Cr condensed primarily as metal its fractionation behavior would be unexplicable. Examination of some coarse grained olivine chondrules in Allende revealed high local concentration of Cr. Submicron sized spherules of a nearly pure Cr mineral ( $\text{Cr}_2\text{O}_3$ ) occur in regular rows suggestive of an exsolution process. Chromium enrichments are also observed along grain boundaries in these chondrules, although no specific minerals could be observed there. The chondrules commonly display reaction rims consisting of fine grained silicates, metal, FeS,  $\text{FeCr}_2\text{O}_4$  and FeS- $\text{FeCr}_2\text{O}_4$  intergrowths. Evidently the Cr situated on grain boundaries was susceptible to further reactions. Several "amoeboid olivine" inclusions were probed also but their Cr contents were negligible. Apparently, olivine condensation was at least a two stage process, one which incorporated no Cr and a second which incorporated most of the Cr.

An attempt has also been made to relate the fractionation of oxygen isotopes observed in chondritic material [5] to the refractory element fractionation. The greatest enrichments of  $\text{O}^{16}$  are known to occur in the refractory-rich inclusions. Seemingly the partial removal of this material could be related to the isotope fractionation pattern observed among the various chondrite groups. However, the oxygen isotope pattern is quite unlike the refractory element pattern. If  $\text{O}^{16}$  is assumed to be the only isotope whose abundance varies the pattern is  $\text{C} < \text{E} < \text{H} < \text{L, LL}$ , quite unlike the refractory element pattern. The resolution of these differences may have an important bearing on the questions the identity and distribution of the  $\text{O}^{16}$  carrier in the solar system.

### References

- (1) Urey, H. C. (1961) J. Geophys. Res. **66**, 1988.
- (2) Larimer, J. W. and Anders, E. (1970) Geochim. Cosmochim. Acta **34**, 367.
- (3) Grossman, L. and Ganapathy, R. (1976) Geochim. Cosmochim. Acta **40**, 331.
- (4) Grossman, L. and Olsen, E. (1974) Geochim. Cosmochim. Acta **34**, 173.
- (5) Clayton, R. N., Onuma, N. and Mayeda, T. (1976) Earth Planet Sci. Lett. **30**, 10.



GRAIN CARRIERS OF ISOTOPIC ANOMALIES, Steven H. Margolis and Sydney W. Falk, Enrico Fermi Institute, Univ. of Chicago, Chicago, IL 60637.

Anomalies in the isotopic abundances of Oxygen [1] and Magnesium [2] as seen in inclusions from the Allende meteorite suggest the presence of material from a supernova in the solar nebula at the time of condensation. In view of studies of grain formation in supernova ejecta [3,4], and suggestions that grains would provide effective carriers for isotopic anomalies [3,4,5], the ability of grains to penetrate the protosolar nebula (carrying material of anomalous composition) has been studied. Within very broad limits, grains moving into the protosolar nebula are stopped in a distance of order

$$L = \frac{m_d}{2\pi a^2 \rho_g}$$

where  $m_d$  is the mass of a grain,  $a$  is the radius of a grain, and  $\rho_g$  is the average gas density ahead of the grain [6,7]. Physically, this corresponds to the distance over which the grain sweeps up a mass of gas equal to its own. It is emphasized that the maximum penetration distance is no greater than a few times the scale  $L$  and proportional to grain radius.

Thus, the distance that a grain can travel is closely tied to the initial configuration of the target gas. For a configuration similar to a standard HI cloud [8] with average density 10 H atoms/cc, the penetration distance for typical grain parameters ( $m_d = 10^{-14}$  g,  $a = 10^{-5}$  cm) is  $\sim 2 \times 10^{18}$  cm. In the absence of other effects, the grains would accumulate throughout a skin layer of thickness about 0.1 times the cloud diameter. This configuration is simply one of a number of target states examined and is used as an example. In all reasonable cases examined thus far, the integrated column density of the target is such that the possible penetration of grains typical of interstellar conditions is limited to a relatively small surface layer. The presence of a magnetic field will further limit grain penetration.

The complete hydrodynamic evolution of a protosolar nebula toward collapse has not been completed. However, detailed studies of the evolution of the edge of a configuration with density at least  $10^{-3}$  atoms/cc have been completed and show the formation of bubbles of gas through Rayleigh-Taylor instabilities of the gas [7]. These bubbles are typically about  $10^{11}$  cm in size; the calculations indicate mixing of these bubbles over scales of several times  $10^{13}$  cm. These results constrain models of the protosolar nebula with similar boundaries which rely on grain carriers of anomalous material. It does appear that such material would be restricted to the edge of the nebula. In order to achieve deeper penetration of the anomalous material and not sacrifice the dilution resistance of the grains, one must postulate deep mixing currents which are so ordered as not to destroy the small bubbles. For such pictures of mixing, this can represent a very strong constraint on the associated turbulence.

## GRAIN CARRIERS

Margolis, S.H.

A class of allowed models involves the formation of the high temperature inclusions at the edge of the protosolar nebula. The calculations discussed here do show temperatures in the edge regions well in excess of the condensation temperatures [ $\approx 2000\text{K}$ ; 9] generally given for the inclusions. Furthermore, sputtering of the grains during penetration rapidly increases the amount of anomalous material in the edge region ready for condensation from the gas. An additional benefit of such models is the obvious means for generating various values of anomalous abundances. A spectrum of grain sizes will provide a gradient of anomalous matter within the edge. These would be small scale effects which might plausibly contribute to the heterogeneity seen in Allende inclusions [10]. Further studies of grain formation [11, 12] in supernova ejecta and the evolution of the nebula [13] should provide stronger constraints on the possible role of grains as carriers of isotopic anomalies.

This work has been supported in part by the National Needs Postdoctoral Fellowship Program and NASA grant NSG-7212 at the University of Chicago.

## REFERENCES

1. Clayton, R.N., Grossman, L. and Mayeda, T.K. 1973, Science **182**, 485.
2. Lee, T., Papanastassiou, D.A. and Wasserburg, G.J. 1977, Ap. J. (Lett.) **211**, L107.
3. Falk, S.W., Lattimer, J.M. and Margolis, S.H. 1977, Nature **270**, 700.
4. Lattimer, J.M., Schramm, D.N. and Grossman, L. 1978, Ap J. **219**, 230.
5. Clayton, D.D. 1975, Nature **257**, 36.
6. Margolis, S.H. 1978, The Moon and Planets, in press.
7. Margolis, S.H. 1978, Ap. J., submitted.
8. Spitzer, L. 1968, Diffuse Matter in Space, (N.Y.: Interscience).
9. Grossman, L. 1972, Geochim. Cosmochim. Acta **36**, 597.
10. Lee, T., Papanastassiou, D.A. and Wasserburg, G.J. 1978, Ap. J. (Lett.) **220**, L21.
11. Lattimer, J.M. and Falk, S.W. 1978, in prep.
12. Margolis, S.H. and Lattimer, J.M. 1978, in progress.
13. Margolis, S.H. 1978, in prep.

DUST IN COSMIC-PLASMA ENVIRONMENTS, D. A. Mendis, Dept. of Applied Physics and Information Science, University of California-San Diego, La Jolla, CA 92093

Cosmic dust is invariably immersed in both a plasma and a radiative environment. Consequently it is charged to some electrostatic potential which depends both on the properties of the environment as well as the nature of the dust. This charging affects both the physical and dynamical properties of the dust. A proper understanding of these effects are required in order to interpret several observed dust phenomena within the solar system.

In this paper we address several aspects of this problem. The important processes controlling the electrical potentials of dust grains in planetary magnetospheres are considered, and the quasi-equilibrium potentials acquired by them in different plasma and radiative environments are evaluated. The orbital dynamics of such charged grains is discussed and it is shown that magneto-gravitational capture is possible for grains with sufficiently large specific charge. This may be the origin of dust rings within the magnetosphere of Jupiter.

The possible break-up of these dust grains when charged to large electrical potentials and its consequences are discussed.

Certain phenomena observed on satellites located within planetary magnetospheres are explained in terms of their interaction with fluxes of charged dust grains.

The cosmogonic significance of dust-plasma interactions is briefly discussed.

# THE OBSERVED INFRARED PROPERTIES OF GRAINS IN SPACE

K. Michael Merrill, University of Minnesota,

Minneapolis, Minnesota 55455

The infrared properties of dust in space, as inferred from infrared observations at low to moderate spectral resolution at wavelengths  $\leq 30\mu\text{m}$  are summarized. Condensates at high temperature: carbon and silicon carbide; moderate temperature: silicates; and low temperature - ices are briefly discussed. Strong band emission from as yet unknown species has been detected in a variety of objects.

High temperature condensates are seen in a variety of objects. The  $11\mu\text{m}$  band of silicon carbide has been identified in the spectra of carbon stars ( $\text{C/O} > 1$ ) and possibly in certain planetary nebulae. Featureless material (no identifying band structure) can be seen in emission in the circumstellar shells of carbon stars, WC9 Wolf-Rayet stars, novae, and planetary nebulae. In all but the latter, the material appears to be continuously formed at a high rate. In particular, shell formation in novae is quite abrupt - once triggered the dust shell forms in a matter of days, rapidly dropping from an initial temperature near 1500K to an apparently self regulated 1000K for hundreds of days until the dust episode finally ends with a gradual decline in grain temperature as the cloud dissipates. For a variety of reasons the featureless material is generally assumed to be some form of carbon. Comet ejecta also show evidence of featureless material which is not necessarily a high temperature condensate.

Silicate grains, usually considered to be intermediate temperature condensates, have been identified in diverse spatial environments on the basis of characteristic infrared emission/absorption band signatures. Silicates are important constituents of the Zodiacal cloud, comets, molecular clouds, compact HII regions and of the general interstellar medium. Mass loss from evolved stars appears to be a significant source of silicate-rich material: the circumstellar envelopes of cool luminous stars with solar composition ( $\text{O/C} > 1$ ) are predominantly silicates. Evidence for silicate absorption is seen in a number of compact planetary nebulae. In addition to the well known stretching and bending modes at  $10\mu\text{m}$  and  $20\mu\text{m}$ , an apparent emission band near  $33\mu\text{m}$  in the spectra of cool stars has been tentatively identified as a lattice vibrational mode in silicates. As seen in comets and to a lesser extent in reflection nebulae, silicates are strongly forward scattering. Evidence that circumstellar silicates

## THE OBS. INF. PROP. OF GRAINS IN SPACE

Merrill, K.M.

possess non-negligible near infrared and visual capacity (unlike their pure crystalline terrestrial counterparts) is based on model fits to the observed behavior of the silicate band with shell optical depth and to reproduce the visibility curves measured by spatial interferometry of cool stars. The remarkable uniformity of the well-studied emission/absorption profile of the  $10\mu\text{m}$  band from source to source together with an apparent lack of sub-structure at higher resolution suggest that the observed profile is intrinsic rather than due to a combination of particle size, shape and composition distributions within the grain population. Recent laboratory experiments have produced several silicate minerals with the necessary spectral characteristics.

To date, evidence for low temperature condensates is confined to detections of characteristic band absorption within the sheltering environment of dense molecular clouds -either as separate grains or as mantles of the grains seen in the general interstellar medium. The strength of the  $3.07\mu$  absorption feature - identified with water ice with possible contributions from ammonia ice - is not correlated with the apparent  $10\mu$  silicate absorption optical depth. The ratio  $\tau_{\text{ice}}/\tau_{\text{silicate}}$  varies from  $\approx 0.03$  in the inter-stellar material up to  $\geq 1$  in certain molecular clouds. Further, the observed strength of the ice band does not correlate with the variation in anomalous extinction across the  $\rho\text{Oph}$  molecular cloud. The  $11\mu\text{m}$  band of water ice has been tentatively identified. A very weak absorption band at  $3.4\mu\text{m}$  (methane ice?) can apparently be seen in clouds with deep water ice bands. Confirmation of this feature as an absorption band is complicated by the existence of a narrow band at  $3.3\mu\text{m}$  in many objects including compact HII regions which are presumably seen embedded within the clouds.

As yet unidentified strong emission features at  $3.3$ ,  $3.4$ ,  $6.3$ ,  $7.8$ ,  $8.6$ ,  $11.3\mu\text{m}$  are seen in certain peculiar stars, planetary nebulae, compact HII regions, ionization fronts and the nuclei of active galaxies under a wide range of excitation and temperature environments. Whether the material is gaseous or solid (or possibly absorbed species on grains) is unknown.



## EXPERIMENT ON THE CLUSTERING OF FINE PARTICLES

T. Onaka, Y. Nakada, and F. Kamiyo  
Dept. of Astronomy, Univ. of Tokyo, Tokyo 113, Japan

### § Introduction

Grain growth by grain-grain collisions is expected in various astrophysical problems [1]. Experiments of the collisions have been limited until now to the high-velocity case [2]. However, thermal collisions will take place in the early stage of the solar nebula. Our purpose is to investigate experimentally the clustering of grains by thermal collisions. Applications of the results to the primordial solar nebula are also discussed.

### § Experimental Procedure

The fine particles are prepared by the so-called gas evaporation method [3]. The work chamber is filled with argon gas of a fixed pressure (Fig. 1). Sample material is put in an alumina-coated tungsten heater. The evaporating gas of the sample material soon cools in the argon air to recondense as small grains. They are collected on specimen grids at different heights above the heater. Micrographs are taken by electron microscope JEM-7A and numbers of grains in each cluster are counted.

In our experiment, silicon is used as sample material. The temperature of the heater is fixed at  $1400^{\circ}\text{C}$ . Two cases of the pressure of argon gas are studied: 5 Torr and 40 Torr. The specimen grids of electron microscope are placed at 3, 4, 5, 6, 7, and 8 cm above the heater.

### § Results and Analysis

#### a) Mass distribution of cluster

Since the size distribution of the prepared grains has small dispersion around the sharp maximum ( $\sim 10\%$ ), the mass of a cluster is assumed to be proportional to the number of grains in it. The mass distribution of cluster is obtained by counting  $n(k)$ , the number fraction of clusters which contain  $k$  grains, on the micrographs (Fig. 2). In Figure 3,  $f(k)$  defined as  $k^2 n(k)$  (instead

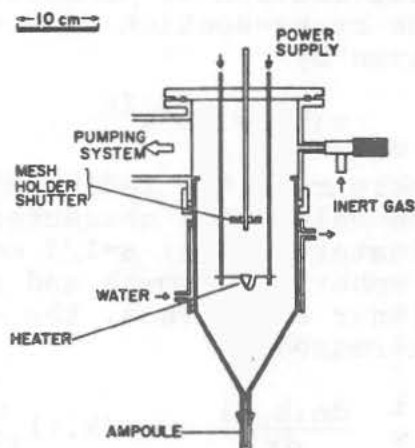


Fig. 1

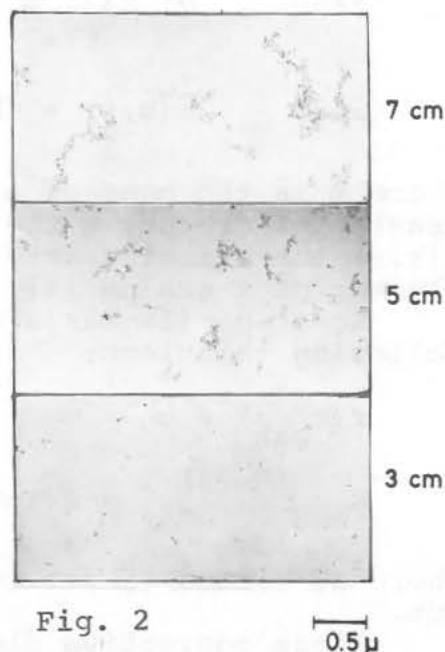


Fig. 2

## CLUSTERING OF FINE PARTICLES

Onaka, T. et al.

of  $n(k)$  is plotted against  $\log k$ . Quantity  $f(k)$  is normalized by  $\int_0^\infty f(k) d(\ln k) = 1$ .

b) Collisional cross-section

To interpret the results, the measured distribution  $f(k)$  is compared with the theoretical one. The method of analysis is summarized briefly as follows.

It is assumed that the velocity distribution is Maxwellian and that the cross-section of a cluster is given by

$$\sigma(k) = \pi r^2 k^{2\beta}, \quad (1)$$

where  $r$  is the radius of a grain.

The value of  $\beta$  characterizes the cluster growth:  $\beta=1/3$  corresponds to a spherical growth and  $\beta=1/2$  to a planar one. Thus, the growth of cluster by mutual collisions is expressed as

$$\frac{dn(k, \tau)}{d\tau} = -n(k, \tau) \sum_{i=1}^{\infty} \alpha(k, i) n(i, \tau) + \frac{1}{2} \sum_{j=1}^{k-1} \alpha(j, k-j) n(j, \tau) n(k-j, \tau) \quad (2)$$

$$\text{with} \quad d\tau = \sqrt{\frac{8\pi k_B T}{M}} n_0 s r^2 dt$$

$$\text{and} \quad \alpha(k, i) = (k^\beta + i^\beta)^2 \left(\frac{1}{k} + \frac{1}{i}\right)^{1/2},$$

where  $M$  is the mass of a grain,  $T$  the temperature,  $n_0$  the number density of grains,  $s$  the sticking probability,  $t$  the time, and  $\alpha(k, i)$  the sticking rate between a cluster of  $k$  grains and a cluster of  $i$  grains [4].

Equation (2) has a similarity solution which gives us the following relations:

$$f(k_{\max}) = c \quad (3)$$

$$k_{\max}^{(3-4\beta)/2} = a(\tau - \tau_0), \quad (4)$$

where  $a$ ,  $c$ , and  $\tau_0$  are constants and at  $k=k_{\max}$   $f(k)$  becomes maximum.

Since convective flow is generated above the heater, the rela-

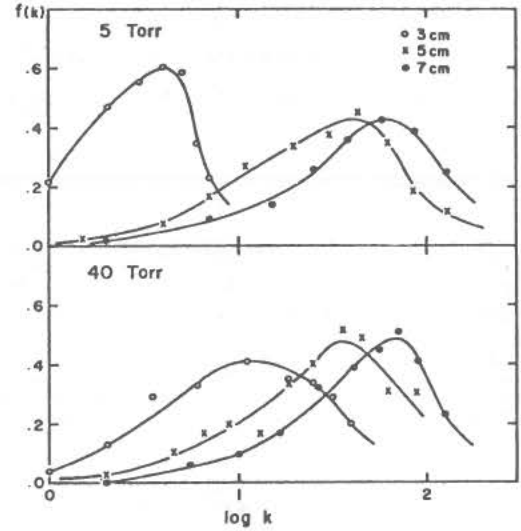


Fig. 3

## CLUSTERING OF FINE PARTICLES

Onaka, T. et al.

tion between the height  $h$  above the heater and the non-dimensional time  $\tau$  is given by

$$d\tau = A dh \quad (5)$$

$$\text{with } A = \sqrt{\frac{8\pi k_B T}{M}} n_0 s r^2 \frac{1}{V_c},$$

where  $V_c$  is the convective velocity. If  $A$  is assumed to be constant over the region of the measurement, Equation (4) is rewritten as

$$k_{\max}^{(3-4\beta)/2} = a'(h-h_0), \quad (6)$$

where  $a'$  and  $h_0$  are constants. Since grain recondensation takes place near the heater ( $<0.5$  cm),  $h_0$  can be neglected.

Under these assumptions,  $\log k_{\max}$  relates linearly to  $\log h$  with the gradient  $2/(3-4\beta)$ . The results of our measurement are shown in Figure 4 for the cases of  $P=5$  Torr and  $P=40$  Torr. Both cases show the linear relations, confirming the validity of the above assumptions. The small dispersion in the figure may be attributed to the experimental errors. The index  $\beta$  is determined to be 0.5 from the gradient, which means that the growth of cluster is planar, and not spherical as usually assumed. The important consequence of the planar growth is a large ratio of surface area to mass (high porosity). Our experiments are limited to rather small cluster ( $k \lesssim 200$ ). It is unlikely that the planar growth continues up to 1 millimeter size. However, we believe that a large ratio of surface area to mass will still hold in the case of large clusters.

## c) Comparison with numerical simulation

In the previous section only the variation of  $k_{\max}$  was used to determine the index  $\beta$ , but neither the peak value  $f(k_{\max})$  nor the half width of the distribution were checked. Equation (2) was solved numerically for the case  $\beta=1/2$  and  $\beta=1/3$ . The distribution  $f(k)$  for  $\beta=1/3$  has a higher peak and a narrower half-width than the experimental one. For  $\beta=1/2$  the

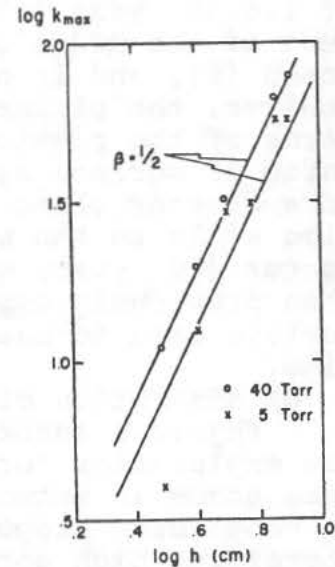


Fig. 4

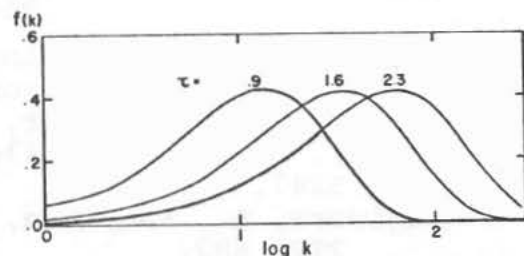


Fig. 5

## CLUSTERING OF FINE PARTICLES

Onaka, T. et al.

shape of the distribution (Fig. 5) is consistent with the experiment.

## § Applications to the Primordial Solar Nebula

The clusters on the micrographs (Fig. 2) show the so-called necklace structure. The planar growth may come from this structure. Though a satisfactory explanation has not been given for the necklace structure, it is very common in grains prepared in the laboratory. It is likely that the primordial clusters of grains had also necklace structure and, therefore, the large ratio of surface area to mass. Two problems of the primordial solar nebula are considered in connection with it.

## a) Scatter in the solidification time

The solidification time indicated by  $^{129}\text{I}/^{127}\text{I}$  has scatter of  $1.5 \times 10^7$  year [5]. This time span cannot be found in any process of the model of the primordial solar nebula previously proposed [6], and is now expected due to the extra-solar origin [7]. However, the planar growth offers an alternative explanation in terms of the previous model of closed system. Since the large ratio of surface area to mass keeps the drag force per unit mass of a cluster close to that of a single grain, the sedimentation time scale to the midplane of the primordial solar nebula becomes longer ( $10^7$  year, which is the time scale for a single grain) than previously expected ( $10^6$  year). Thus, the large ratio of surface area to mass can explain the scatter in the solidification time.

## b) Adsorption of rare gases on grains

Physical adsorption mechanism has been proposed as a possible explanation for the origin of the 'planetary' component of rare gases in meteorites. The total amounts of adsorbed material is considered proportional to the surface area of adsorber. Therefore, high porosity, which is indicated by the adsorption experiment of meteorites, is required to explain their large amounts in meteorites. Such high porosity is also suggested by the planar growth, which will leave the large effective surface area for adsorption on the cluster of grains.

## References

- [1] Salpeter, E.E. 1977, *Ann. Rev. Astron. Astrophys.* 15, 267.  
Scalo, J.M. 1977, *Astron. Astrophys.* 55, 253.
- [2] Kerridge, J.F., Vedder, J.F. 1972, *Science* 177, 161.  
Vedder, J.F., Mandeville, J.C. 1974, *J. Geophys. Res.* 79, 3247.  
Fujiwara, A., Kamimoto, G. and Tsukamoto, S. 1978, *Nature* 272, 602.
- [3] Yatsuya, S., Kusakabe, S., Uyeda, R. 1973, *Japan J. Appl. Phys.* 13, 1001.  
Hayashi, T., Ohno, T., Yatsuya, S., Uyeda, R. 1977, *ibid.* 16,

## CLUSTERING OF FINE PARTICLES

Onaka, T. et al.

705.

- Lefèvre, J. 1970, *Astron. Astrophys.* 5, 37.  
 Codina-Landaberry, S., Marcondes-Machado, J.A., Magalhães, A.M. 1976, *Astron. Astrophys.* 49, 407.  
 Kamijo, F., Nakada, Y., Iguchi, T., Fujimoto, M.-K., Takada, M. 1975, *Icarus* 26, 102.
- [4] Safronov, V.S. 1972, "Evolution of the Protoplanetary Cloud and Formation of the Earth and the Planets" (Israel Program for Science Translations, Jerusalem), Chap. 8.  
 Hayashi, C., Nakagawa, Y. 1975, *Prog. Theor. Phys.* 54, 93.
- [5] Podosek, F.A. 1970, *Geochim. Cosmochim. Acta* 34, 341.
- [6] Alfvén, H., Arrhenius, G. 1974, *Astrophys. Space Sci.* 29, 63.  
 Cameron, A.G.W. 1973, *Icarus* 18, 407.  
 ———. 1975, *ibid.* 24, 128.  
 Kusaka, T., Nakano, T., Hayashi, C. 1970, *Prog. Theor. Phys.* 44, 1580.
- [7] Clayton, D.D. 1975, *Astrophys. J.* 199, 765.  
 Cameron, A.G.W., Truran, J.W. 1976, *Icarus* 30, 447.  
 Lattimer, J.M., Schramm, D.N., Grossman, L. 1978, *Astrophys. J.* 219, 230.
- [8] Fannale, F.P., Cannon, W.A. 1971, *Geochim. Cosmochim. Acta* 41, 195.



## COMPUTER SIMULATION AND THE STUDY OF CONDENSATION

M. Rao and B.J. Berne

Chemistry Department

Columbia University, New York, N.Y. 10027

Computer simulation is used to study the kinetics of condensation from a gas phase. The formation of nuclei from the supersaturated vapor is observed in both Monte Carlo and Molecular Dynamics simulations, in an argon like fluid. The nuclei correspond to both liquid and solid like droplets depending on the ambient temperature. The droplets grow in essentially adiabatic conditions; that is, collisions of the nuclei with vapor are sufficiently infrequent that due to latent heat effects the temperature of the droplet increases.

The classical nucleation theory is modified for finite systems, taking into account gas imperfection. The size of both the critical cluster and the equilibrium droplet are discussed in this context.

## INFRARED STUDIES OF SILICATES

Louis A. Rose<sup>\*</sup>

Laboratory for High Energy Astrophysics  
NASA/Goddard Space Flight Center  
Greenbelt, Maryland 20771

The identification of a 10  $\mu\text{m}$  emission feature in the energy spectra of M stars (1) has prompted a large amount of study to understand the composition and structure of materials that produce this feature. It is believed that silicate grains are the source of the astrophysical 10  $\mu\text{m}$  feature because they have an absorption band near 10  $\mu\text{m}$  due to Si-O stretching motions (2).

A great deal of experimental work has been done in studying infrared spectra of silicates in the forms of powders, polished plates and single grains (3,2,4,5). Logan and Hunt (6) acquired infrared emission spectra of silicates under simulated lunar conditions; studies of terrestrial, meteoritic and synthetic materials, aimed specifically at understanding the astrophysical 10  $\mu\text{m}$  features, have been conducted by Zaikowski *et al.* (7) and by Day (8). A number of theoretical studies have been done to gain information about silicate dust grains. If the complex refractive index of a mineral as a function of wavelength is known, Mie theory calculations can be performed for small grains of these minerals. By comparing calculated spectra to the infrared spectra of Martian dust, Toon *et al.* (9) have derived information concerning particle size distribution and dust composition.

In this work, which is experimental in nature, optically thin samples of fine grain silicates were studied in the 7-14  $\mu\text{m}$  range using intermediate resolution emission and absorption spectroscopy. Experimental techniques that imitate telescope observations and which are similar to the methods employed by Hunt and Logan (5) were used to obtain emission spectra. Samples were prepared by depositing grains, one layer thick, on low-emissivity substrates. For most samples the grains were in the size range 0-2  $\mu\text{m}$  so that the variation of emissivity with wavelength of individual grains could be seen.

A comparison of the results obtained using crystalline and amorphous material show that amorphous silicates more nearly simulate the smooth 10  $\mu\text{m}$  feature seen in emission in the spectra of Comet Kohoutek (10) and in absorption in such objects as the Becklin-Neugebauer-Kleinman-Low complex in Orion (11). Conclusions are drawn concerning the composition of materials that would produce spectra to match the intermediate resolution spectra of Comet Kohoutek (10).

---

<sup>\*</sup>NAS/NRC Research Associate

## INFRARED STUDIES OF SILICATES

Louis A. Rose

## REFERENCES

1. Woolf, N. J. and Ney, E. P., Ap. J. (Letters) 155, L181 (1969).
2. Hunt, G. R. and Salisbury, J. W., Mid-Infrared Spectral Behavior of Igneous Rocks (Air Force Cambridge Research Laboratories, Report Number AFCRL-TR-74-0625) (1974).
3. Pfund, A. H., Journal of the Optical Society of America 23, 375 (1933).
4. Lyon, R.V.P., Evaluation of Infrared Spectrophotometry For Compositional Analysis of Lunar and Planetary Sails, Part II: Rough and Powdered Surfaces, NASA Contractor Report CR-100 (1964).
5. Hunt, G. R. and Logan, L. M., Applied Optics 11, 142 (1972).
6. Logan, L. M. and Hunt, G. R., Journal of Geophysical Research 75, 6539 (1970).
7. Zaikowski, A., Knacke, R. F., and Porco, C. C., Astrophysics and Space Science 35, 97 (1975).
8. Day, K. L., Ap. J. (Letters) 192, L15 (1974).
9. Toon, O. B., Pollack, J. B. and Sagen, C., Icarus 30, 663 (1977).
10. Merrill, K. M., Icarus 23, 566 (1974).
11. Gillett, F. C. and Forrest, W. V., Ap. J. 179, 483 (1973).

FORMATION OF  $H_2$  ON AMORPHOUS INTERSTELLAR ICE GRAINS, R. Smoluchowski  
Department of Astronomy, University of Texas, Austin, TX. 78712

The presence of icy grains in space has been discussed for many years and, although there is plenty of evidence for other grains, icy grains (and ice covered grains) are probably the most studied interstellar solid material. In particular the problem of accounting for the formation of  $H_2$  molecules out of H atoms on the surface of grains has been studied in detail for ice surfaces. The basic theoretical studies of this process have been made by E. E. Salpeter and his collaborators (1,2,3,4,5) using a rather simple model in which the ice was assumed to have a cubic structure which provided a distance of 3 Å between nearest equivalent sites at which H atoms could be adsorbed. They used a Lennard-Jones potential between  $H_2$  and H with suitably chosen binding energy and the separation parameter. The important result of the theory is the conclusion that, at the low temperatures, an adsorbed H atom can be described by a wave function which spreads rapidly over the crystallographically perfect grain surface forming a band (analogous to those which exist in metals) so that the interaction with another H atom, similarly adsorbed at another site, is essentially instantaneous. The rate of formation of free  $H_2$  molecules is thus controlled by the life time of the adsorbed atoms, by the probability that another atom is adsorbed on another part of the same grain during this time and by the desorption rate of the  $H_2$  molecules. Correction for various defects and atomic irregularities were also introduced.

The purpose of this paper is to point out the differences which occur if one admits the possibility that the icy grains (or the icy cover of non-icy kernels) are not crystalline but amorphous (6). Experiments indicate (7,8) that  $H_2O$  condensing slowly below 150°K is amorphous (actually there is another more dense amorphous structure near 10°K) so that unless the grains were initially formed at higher circumstellar temperatures they should be amorphous. The probability that interstellar radiation and temperature fluctuations can lead to crystallization of the initially amorphous grain appears to be very low.

Before analyzing the rate of  $H_2$  formation on the metastable amorphous ice grains, the classical calculations for crystalline ice were repeated using the actual structure of the normal stable hexagonal ice and using an interaction potential based on recent experimental and theoretical data from which the repulsive and attractive forces can be deduced. The main difference turns out to be the fact that the distance between equivalent sites is 4.5 rather than 3 Å so that the band is much narrower and the spread of the wave function less rapid. Nevertheless the interaction of two adsorbed H atoms is still essentially instantaneous and the rate  $H_2$  formation is controlled by the same factors as in Salpeter's theory.

The situation changes drastically when amorphous ice is considered. Assuming that each adsorbed H atom is in contact with at least three  $H_2O$  molecules of the surface the interaction has to be summed over the various possible configurations of the rest of the random neighborhood. This leads to

## AMORPHOUS ICE

R. Smoluchowski

a range of adsorption energies which are randomly distributed over the surface. As a result, at low temperatures, only localized states are formed and there is no long-range migration of the adsorbed atoms. The situation is entirely analogous to the well known, and complicated, problem of the binding and mobility of charge carriers in amorphous semiconductors (9,10). With increasing temperature the adsorbed H atom can reach neighboring states of progressively higher energy so that eventually long-range paths on the surface are permitted. This aspect of the problem uses the well known results and formulation of the percolation theory.

The negligible mobility of H atoms adsorbed on amorphous surfaces has profound consequences for the formation of  $H_2$  molecules because an H atom localized somewhere on a surface could interact with another H atom only if it happened to be adsorbed within a few intermolecular spacings from it. Thus not only the probability of  $H_2$  formation would be very low but it would be essentially independent of the radius of the grain in contrast to the situation for crystalline ice where the probability is proportional to the surface of the grain. The broad range of adsorption energies implies a broad range of life times of the H atoms on the surface and the need for high frequency of impingement of H atoms which means high density HI regions. With increasing temperature the probability of recombination would increase since the mobility should go up as  $\exp[-T_0/T]^{1/4}$  where  $T_0$  is a parameter characterising the amorphous surface. A detailed quantitative evaluation of the model is rather difficult because of the remaining uncertainty about the best effective H- $H_2O$  interaction potential. Furthermore the question of the stability of the amorphous ice in an interstellar radiative ambience including the fact that its thermal conductivity is 50 to 100 times lower than that of the crystalline ice has as yet not been considered in sufficient detail. It should be added that the probability of a diffusive penetration of an adsorbed H atom into the ice grain using the so-called Bjerrum-defects in crystalline ice or intermolecular spaces in amorphous ice turns out to be negligible. A potentially important consequence of the amorphous nature of ice grains is the fact that they would be expected to absorb ultraviolet radiation of somewhat longer wave-lengths than crystalline ice which is essentially transparent near the cut-off of the interstellar ultraviolet spectrum. Since the intensity of this radiation increases rapidly before the cut-off the amorphous grains would be more likely ionized and could have higher temperatures than crystalline grains. It should be stressed that the amorphous solids here discussed differ fundamentally from strongly irradiated crystalline solids because the latter retain their essential periodic structure and are not random.

Supported by NASA grant, NSG-7283 Sup.1



## AMORPHOUS ICE

R. Smoluchowski

1. D. Hollenbach and E. E. Salpeter, J.Chem.Phys. 53, 79 (1970) and Astroph.J. 163, 155 (1971).
2. W. D. Watson and E. E. Salpeter, Astroph.J. 174, 321 (1972) and 175, 659 (1972).
3. E. E. Salpeter and W. D. Watson, IAU Symposium #52, p. 369, 1973.
4. W. D. Watson in "Atomic and Molecular Physics and the Interstellar Matter", Les Houches Aug. 1974, Ed: R. Balion, P. Encrenaz and J. Lequeux, American Elsevier Publ. Co., New York, N.Y. 1975.
5. W. D. Watson, Rev. Mod. Phys. 48, 413 (1976).
6. R. Smoluchowski in "Comets, Asteroids and Meteorites" IAU Colloq. #39 Lyon 1976, Ed: A. H. Delsemme, U. of Toledo Press, Toledo, Ohio 1977.
7. A. H. Narten, C. G. Venkatesh and S. A. Rice, J. Chem. Phys. 64, 1106 (1976).
8. P. V. Hobbs "Ice Physics", Clarendon Press, Oxford 1974.
9. N. F. Mott and E. A. Davis "Electronic Properties of Non-Crystalline Materials" Oxford U. Press, Oxford 1971.
10. J. Tauc "Amorphous and Liquid Semiconductors", Plenum Co., New York, N.Y. 1974.

EFFECT OF VARIED CHEMICAL COMPOSITION, GRAIN MORPHOLOGY, AND  
CHEMICAL SPECIATION ON THE 4-14 MICRON SPECTRA OF LABORATORY GRAIN SYSTEMS;  
John R. Stephens, Chemistry Department, Univ. of Calif., San Diego, La Jolla,  
Calif., 92093.

The results of equilibrium thermodynamic calculations dealing with the stability of solids under conditions believed to be characteristic of protoplanetary nebulae (1) and stellar atmospheres and circumstellar shells (2) are generally in agreement with the major phases which occur in meteorites (3), and cosmic grain materials, particularly silicates (4) and silicon carbide (5), which infrared spectra suggests occurs as submicron-sized grains in astronomical environments. Equilibrium thermodynamic calculations, however, are not capable of predicting the morphology, size, existence of multi-component grains, or metastable phases present in cosmic grain systems. Since these parameters effect the spectral signature of grain systems (6), laboratory studies dealing with the condensation behavior of cosmically abundant elements combined with spectral studies of grains produced are needed to provide a basis for the interpretation of astronomical spectra. Spectral studies of laboratory grain systems are particularly useful in establishing the sensitivity of emission or absorption features to the structural, chemical, and morphological characteristics of the grains which give rise to the feature. Presented here are absorption (extinction) and emission spectra of laboratory silicate grain systems. The effect of varied chemical composition, crystal structure, and grain morphology on the spectra from 4 to 14 microns is examined. A review of our laboratory condensation experiments and application of the results to the formation of meteorites is discussed in an accompanying paper presented by B. K. Kothari.

Laboratory grain systems were produced by vaporizing a portion of a solid mineral target in a controlled atmosphere by a series of pulses from a solid state laser. The material vaporized from the target recondenses into strings of grains which have a median diameter of 15-30 nm. The condensate smoke settles out into scanning and transmission electron microscope sample holders and KBr disks for absorption or a copper block for emission analyses. The morphology, diffracting structure, and approximate chemical composition are determined by electron microscopy, electron diffraction, and energy dispersive microprobe analysis. Details of the experimental and analytical procedures are given elsewhere (7, 8). Scanning and transmission electron micrographs of an amorphous silicate condensate of approximately olivine composition produced by vaporizing olivine in O<sub>2</sub> are shown in Figure 1a and b. The condensed grains occur as tangled chains of spherical submicron particles, with the chains extending over many microns. The grains are single phased and produce only a diffuse electron diffraction pattern, which is due to the glassy structure of the condensate. By vaporizing the minerals in an O<sub>2</sub>, H<sub>2</sub> or Ar atmosphere, oxidizing, reducing or inert conditions may be established during condensation and some control exercised on the phases present in the condensate.

## EFFECT OF VARIED CHEMICAL COMPOSITION -----

Stephens, J. R.

Infrared absorption and in some cases emission spectra were taken of  $\sim 10 \mu\text{m}$  thick, optically thin ( $\leq 10\%$  absorbing) layers of condensate on KBr disks or copper substrates. Some of the spectra presented here are discussed elsewhere (9). Table 1 summarizes the condensate systems for which infrared spectra have been obtained in this study, including the composition of the targets and the conditions of the experiments. The important morphological, chemical and structural characteristics of the condensates are: 1. The condensates always occur as strands of submicron grains. 2. Silicate condensates which are produced by vaporizing silicate minerals in oxygen produce homogeneous, glassy condensates, while silicates vaporized in a reducing atmosphere produce multiphase grains consisting of glass and reduced metal phases ( $\alpha\text{Fe}$  and  $\text{FeSi}$ ). The multiphased metal-silicate condensates have a structure similar to that proposed by Nandy and Wickramasinghe (10). 3. The approximate chemical composition of the condensates were within 30% of the target mineral in each case. The olivine and pyroxene condensates are clearly distinguishable by their  $\frac{\text{Fe} + \text{Mg}}{\text{Si}}$  ratios.

A detailed discussion of the possible similarities between our laboratory condensate systems and cosmic grains of a number of phases predicted to condense in astronomical environments including C,  $\text{Al}_2\text{O}_3$ , SiC, Ni-Fe alloy, and silicates is given elsewhere (7).

Infrared absorption and emission of the glassy olivine and pyroxene condensates show features which are distinctly different from the corresponding crystalline minerals (9). The bandcenter of the " $10 \mu\text{m}$  silicate feature" is dependent on the composition of the condensate, and ranges from 9.75 (olivine condensate) to 9.0 microns (amorphous  $\text{SiO}_2$ ). The olivine condensate gives the best fit to the 9.7  $\mu\text{m}$  bandcenter of the astronomical " $10 \mu\text{m}$ " feature. Differences between the absorption (extinction) and emission spectral profiles represent the scattering contribution to the extinction, and show characteristic features which may allow information to be obtained on the size and morphology of cosmic grains. The 4-14 micron spectrum of the multiphased glass and metal olivine condensate shows weak peaks at 6.2 and 7.0 microns in addition to the 9.75 micron silicate peak. The differences in the spectra may provide a tool to study the chemical speciation occurring in astronomical grain systems.

ACKNOWLEDGMENT

I wish to thank R. W. Russell for his assistance in taking some of the spectra and allowing the results of the emission studies to be used prior to publication.

REFERENCES

1. Grossman, L. and Larimer, J. W. 1974, Rev. Geophys. Space Phys. 12, 71.
2. Merrill, K. M. and Stein, W. A. 1976, Pub. Astron. Soc. Pacific, 88, 874.
3. Wasson, J. T. 1974, Meteoritics, Springer-Verlag, New York, 46.
4. Ney, E. P. 1977, Science, 195, 541.
5. Hackwell, J. A. 1971, Ph.D. Thesis, University College, London.
6. Huffman, D. R. 1977, Advances in Physics, 26, 129.

## EFFECT OF VARIED CHEMICAL COMPOSITION -----

Stephens, J. R.

7. Stephens, J. R. and Kothari, B. K. 1978, The Moon and The Planets (in press).
8. Stephens, J. R. and Kothari, B. K. 1978 (in preparation).
9. Stephens, J. R. and Russell, R. W. 1978 (submitted for publication)
10. Nandy, K. and Wickramasinghe, N. C. 1973, Astrophys. and Space Sci.,  
23, 51.

Figure 1 - Olivine Condensate

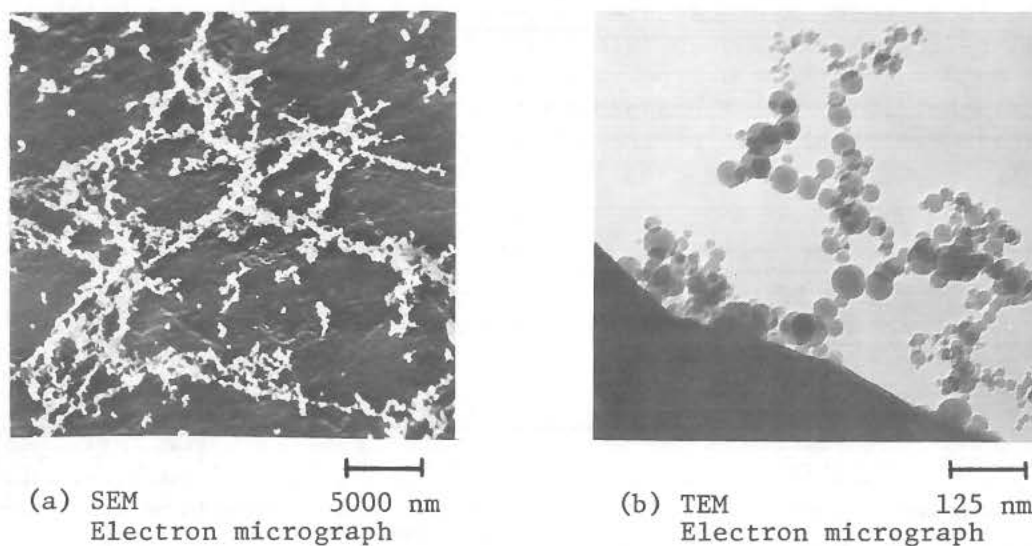


Table 1

Summary of the Systems Studied

Target	Ambient Gas (1 atm)	Electron Diffraction	Median * Size (nm)	Shape
Olivine (Mg <sub>0.9</sub> Fe <sub>0.1</sub> ) <sub>2</sub> SiO <sub>4</sub>	O <sub>2</sub>	Glass	~20	Spherical
	Ar, H <sub>2</sub>	Fe metal + glass	~15-20	Spherical
Pyroxene (Mg <sub>0.9</sub> Fe <sub>0.1</sub> )SiO <sub>3</sub>	O <sub>2</sub>	Glass	~20	Spherical
	Ar, H <sub>2</sub>	FeSi alloy + glass	~15	Spherical

\*Different areas of the same condensate yield median sizes varying by as much as 50%.

# THE ALLENDE METEORITE: AN ASSEMBLAGE OF COSMIC GRAINS

D.A. Wark\*, Geology Department, University of Melbourne, Parkville 3052, Australia.

The Allende meteorite consists of an assemblage of millimeter to centimeter-sized bodies set in an extremely fine-grained black matrix [1]. The bodies include Ca-Al-rich inclusions (CAI's) [2], amoeboid olivine and other fine-grained inclusions [3], and chondrules of olivine, pyroxene and sulfides. The striking differences in the textures and chemical and isotopic compositions of each of these components bespeak of their separate origins and existence as "cosmic grains" before they were brought together in the present meteorite. Many of their original features have survived accretion, compaction and mild metamorphism of the meteorite.

Most of the components can be arranged into the following order of deposition from earliest to latest on the basis of which components have enclosed which [4]: 1. coarse-grained CAI's 2. fine-grained alkali-rich CAI's (Type F) 3. fine-grained alkali-olivine aggregates (Type FAO) [4] 4. amoeboid olivine aggregates (Type AO) 5. olivine chondrules 6. sulfide chondrules 7. matrix.

It is significant that this depositional, or stratigraphic, sequence correlates well with other evidences for the relative times of formation such as: (a) oxygen isotopic compositions become progressively more "normal" (solar) and less  $^{16}\text{O}$ -rich with time [5]; (b) the only two samples known to possess several isotopic anomalies (in Ba, Ca, Mg, Nd and Sr) are coarse-grained CAI's at the start of the depositional sequence; this is consistent with suggested early incomplete mixing of contributions from different nucleosynthetic sources [6]; (c) most coarse-grained CAI's are approximately uniformly enriched over solar abundances in all the most refractory elements without regard to chemical behavior and this is most plausibly due to early condensation from unfractionated, undepleted solar nebula gas. This contrasts with the strongly depleted and fractionated refractory element contents of the later fine-grained CAI's [7]; (d) some coarse-grained CAI's contain  $\mu\text{m}$ -size metal nuggets [8] in which the normally incompatible refractory (Mo, Re, W) and platinum (Pt, Os, Ir, Ru, Rh) metals (RPM's) are alloyed together in solar ratio to one another. Because this is very unlikely by the usual geochemical processes, it strongly suggests early condensation of these RPM nuggets direct from unfractionated gas, as "cosmic grains."

At first sight the diverse Allende components, and particularly the fine-grained materials, appear to represent an impossibly complicated sampling of early solar nebula times and places. Substantial differences occur even between samples of nominally the same type, e.g. some Type A [4] coarse-grained CAI's contain no metal grains while other Type A's may have an abundance of RPM nuggets or of Ni-Fe grains. However, detailed

\*Present address: The Lunatic Asylum, Div. of Geological and Planetary Sciences, Caltech, Pasadena, CA 91125.



## THE ALLENDE METEORITE

D.A. Wark

microscopic and SEM work has uncovered a few useful generalizations signposting this jungle:

(a) Type A, B and I coarse-grained CAI's each have their own kinds of rims with which they terminated their growth, e.g. Type A's were all rimmed with the following set of layers [10], each set being virtually identical in order, composition, texture, and thickness: Fe-rich spinel, nepheline + anorthite + sodalite + olivine, Ti-Al-rich pyroxene, diopside, hedenbergite and, on the outside, andradite. CAI's of Types I and B have rims that are similar to, yet distinct from, those of Type A CAI's [2]. Thus the different coarse CAI types were kept apart until after the rimming process ended.

(b) Many alkali-rich fine-grained CAI's (Type F) are aggregates of myriads of 5 - 50  $\mu\text{m}$  cosmic grains each composed of essentially the same mineral layers as the Type A rims [10]. Thus Type F's are equivalent to Type A rims. Pyroxenes and spinels from Type F's and from the interiors of the coarse CAI's are both enriched similarly in  $^{16}\text{O}$  [5]. Hence Type F's, and presumably rims, both formed in a  $^{16}\text{O}$ -rich environment before the coarse CAI's underwent the selective alteration of melilite and anorthite that has been proposed [11, 12] to account for the co-existence of these minerals (now of "normal" solar oxygen isotopic composition) alongside  $^{16}\text{O}$ -rich spinel and pyroxene.

(c) Deposition proceeded inexorably in one direction and random turbulence had little control over which components became encapsulated within which. However, minor reversals have been noted, e.g. the four concentric zones making up fine-grained inclusion 3598 are, from the inside, Types F, FA0, A0, then back to Type FA0. More serious exceptions include those rare coarse-grained CAI's that possess depleted and fractionated trace element patterns of Type F's, and their converse, the rare fine-grained alkali-rich inclusions that are extremely enriched in refractory elements [13].

(d) The observed samples never represent more than a short part of the whole deposition sequence so that condensed materials were soon isolated from wherever condensation was taking place.

(e) From the strong  $\mu\text{m}$ -scale zonation, sharp concentration gradients [10] and the failure of the Rare Earth Elements to redistribute among the various phases in the fine-grained inclusions [14], it appears that condensation was too rapid and the temperature too low for equilibrium to be attained.

(f) Where the Type F inclusions are aggregates of separate cosmic bodies, the bodies consist of only a single cycle of spinel/feldspathoids/pyroxene. Hence condensation was either stop-start or else the bodies were whisked away to a non-condensing region. The bodies were also either size-sorted or else aggregated rapidly after condensation, before different sizes could mix. However in those Type F inclusions that have "glued" textures [4] condensation and aggregation must have been simultaneous.

(g) The zonation in the fine-grained aggregates shows that there were repeated cycles of condensation of the same phases as those reported above for the rims--only the proportions of these phases changed with time to

## THE ALLENDE METEORITE

D.A. Wark

produce the various later Allende components. In particular the amount of olivine progressively increased from Type F  $\rightarrow$  FAO  $\rightarrow$  AO.

Many of the  $\mu\text{m}$ - and sub- $\mu\text{m}$  RPM nuggets (RPMN's) found in the coarse-grained Allende CAI's undoubtedly pre-existed their hosts as cosmic grains and, because of their very refractory compositions, could be the most ancient solar system condensates or could even be presolar grains as originally suggested by [8]. RPMN's occur in several distinct forms and debate now centers over which forms are the most ancient. The form that RPMN's take seems to be correlated with the Type of the host CAI. Thus the only RPMN's found in Type A CAI's are apparently simple, single-phase alloy grains up to  $3\mu\text{m}$  most of whose compositions have approximately chondritic (solar) RPM element ratios (e.g. 1 and 2, Table 1). A few maverick nugget compositions occur (e.g. 3 and 4, Table 1) but even they mostly have solar Os: Ir: Ru and Pt: Mo: W ratios; only the proportions of these two triads to one another vary, as if the nuggets were microcrystalline 2-phase alloys. Interestingly, each melilite host crystal may have its own unique brand of RPMN though there is not enough data to be sure. If true it would mean (i) that the melilite crystals which make up most of the CAI incorporated the RPMN's very soon after the latter had reached their present sizes and compositions and before dissimilar RPMN's could mix. This would rule out the present RPMN's as interstellar grains although they might have nucleated about interstellar grains; (ii) that RPMN's and their host CAI's formed from the same  $^{16}\text{O}$ -rich (supernova-ejecta-contaminated?) material [15]. Many Type A CAI's that are composed of the most refractory melilite contain no RPMN's, Ni-Fe or other opaque grains which might perhaps also be due to supernova-associated radiation selectively vaporizing opaque grains [16].

RPMN's in Type I CAI's differ from those in Type A CAI's in being multiphase, with Rh and Ru tending to enrich one phase and Pt and Mo the other. Although individual Type I RPMN compositions (5-8, Table 1) scatter more than in Type A, the average RPM ratios are also solar. The coarser phase separation may result from annealing or reheating for which the host silicates show some evidence.

Without pictures it is difficult to comprehend the fantastic variety seen among opaque grains in Type B CAI's. Ni-Fe metal and/or oxides and/or sulfides are very common; so are multiphase RPMN's whose compositions appear to contain almost any permutation of RPMN's, Fe, Ni, Co, V or Ge alloys (9-12, Table 1). But most characteristic of Type B CAI's are the complex bodies up to  $\sim 50\mu\text{m}$  in size composed of intergrown Ni-Fe, sulfides, oxides, Ca phosphate, silicates and assorted  $\mu\text{m}$ -size RPM grains [17, 18]. One school suggests that the oxides, sulfides and complex bodies with their RPMN's are secondary in origin--the products of reaction of very abundant primary RPM, Ge, Co, etc.-bearing Ni-Fe alloys within the Type B CAI's. This school points to the terrestrial occurrence of very similar complex RPM-bearing bodies [19], to the pervasive network of cracks (both open and healed) in Type B's and to other evidences of reaction summarized in [17]. The other school adopts the fundamentally opposite view that the complex

## THE ALLENDE METEORITE

D.A. Wark

RPM bodies are presolar cosmic grains that were incorporated at relatively low temperatures into Type B CAI's [18].

The Allende matrix appears to be a good example of an aggregate of equilibrium-condensed cosmic grains. In the SEM it resembles a random heap of matchsticks, with each "matchstick" being an unzoned euhedral olivine lath of average size approximately  $2 \times 10 \mu\text{m}$  (coarser when further than about  $50 \mu\text{m}$  from the edge of inclusions). Adhering to some of the laths are scattered  $\mu\text{m}$ -size blebs of nepheline, Ni-Fe and Fe-Ni-S, the latter often enclosing cores of the metal. All of these phases have quite constant compositions, as follows (in weight percent): metal Fe 27, Ni 73; sulfide Fe 43, Ni 22, S 35; olivine  $\text{SiO}_2$  36, MgO 24-28, FeO 34-39. These phases must have been already equilibrated before they accreted. If they had equilibrated in situ, so ought the amoeboid olivine aggregates which, however, remain distinctly unequilibrated. Similarly each unzoned olivine chondrule could not have attained its internal homogeneity in situ but before accretion must have undergone prolonged annealing as a "cosmic grain."

Acknowledgements: I thank John Lovering for generously making available his Allende samples and for supporting the M.U.G.D. SEM work via the Australian Research Grants Committee.

References: (1) Clarke et al. (1969); (2) Wark and Lovering (1978), LPS IX, 1211; (3) Grossman and Steele (1976), GCA 40, 149; (4) Wark (1978), LPS IX, 1208; (5) Clayton et al. (1977), EPSL 34, 209; (6) Papanastassiou et al. (1978), LPS IX, 859; (7) Grossman et al. (1977), GLA 41, 1647; (8) Wark and Lovering (1976), LS VII, 912; (9) Grossman (1975), GCA 39, 433; (10) Wark and Lovering (1977), Proc. LSC VIII, 95; (11) Wasserburg et al. (1977), GRL 4, 1; (12) Clayton and Mayeda (1977), GRL 4, 7; (13) Mason and Martin (1977), Smith. Cont. Earth Sc. 19, 84; (14) Nagasawa et al. (1977), GCA 41, 1587; (15) Herbst and Assousa (1977), LS VIII, 427; (16) Falk and Scalo (1975), At. J. 202, 690; (17) Wark and Lovering (1978), LPS IX, 1214; (18) El Goresy et al. (1978), LPS IX, 282; (19) Snetsinger (1973), Am. Min. 58, 189.

## THE ALLENDE METEORITE

D.A. Wark

TABLE 1. Composition of RPMN's in Allende CAI's  
(Wt.Percent; Normalized to Sum 100)

	1	2	3	4	5	6	7	8	9	10	11	12
Fe	6.0	10.0	4.0	64.3	11.7	7.9	5.1	3.3	-	-	-	12.3
Ni	0.8	0.9	1.5	2.2	14.2	0.4	10.6	7.2	-	-	-	18.8
Ge	-	-	-	-	-	-	-	-	-	-	28.4	-
Mo	20.5	23.1	3.6	4.2	28.2	49.2	17.7	6.9	14.9	1.5	-	1.2
Ru	14.8	17.0	43.0	10.9	13.2	-	10.1	17.3	9.9	-	-	20.2
Rh	2.5	-	-	-	-	26.1	-	13.4	-	1.1	3.0	-
W	3.5	2.4	1.1	0.8	-	3.3	-	-	6.2	0.4	13.1	-
Re	1.1	-	-	-	-	-	-	-	5.9	0.9	8.3	-
Os	9.7	9.9	18.1	4.8	7.1	2.7	3.2	8.3	33.9	1.4	14.3	45.5
Ir	11.5	11.5	20.4	4.2	10.5	2.2	10.0	8.6	29.3	11.3	7.4	1.8
Pt	29.6	21.8	4.9	4.9	15.1	8.0	43.2	34.9	-	83.1	25.4	-

(NOTE: Phases 5 and 6 coexist in one RPMN, 7 and 8 in another)

RECOMBINATION DYNAMICS FOR H-ATOMS ON SURFACES OF GRAINS, William D. Watson and Deirdre A. Hunter, Departments of Physics and Astronomy, University of Illinois at Urbana-Champaign, Urbana, Ill. 61801

Trajectories based on classical mechanics are computed for recombining  $H_2$  molecules on rigid surfaces. Monte Carlo sampling of initial locations and velocities is utilized to obtain the average translational energy per molecule formed and the average rotational state of the molecules that escape. Various values for the adsorption energy are considered. In the limit of pure physical adsorption, the average translational energy is about 0.2 eV and the average rotational state is greater than  $J=7$ . Since transfer of energy into the surface is not included, the calculations here are expected to yield upper limits to the actual energies after recombination on interstellar dust grains. Heating of the gas in interstellar clouds by energy from  $H_2$  recombination is thus less significant than might be supposed. The calculations do support the proposal that  $\tilde{\nu}$  recombination contributes to the observed abundances of  $H_2$  molecules in the  $J > 4$  states.



UNIDENTIFIED INFRARED SPECTRAL FEATURES. S. P. Willner, R. C. Puetter, R. W. Russell, Univ. of Calif., San Diego, and B. T. Soifer, Calif. Inst. of Technology.

The infrared spectra between 2 and 13  $\mu\text{m}$  of a variety of objects have become available in the past few years. These spectra have shown many objects to have up to six emission features, which are still unidentified. Other objects show absorptions due to ice, carbon monoxide, silicates, and two unidentified features. The observational characteristics of the unidentified features are discussed here.

The emission features were all discovered in NGC 7027, though at different times and by different observers. The infrared spectrum of this high-excitation planetary nebula is shown in Figure 1 [1]. From 2 to 3  $\mu\text{m}$

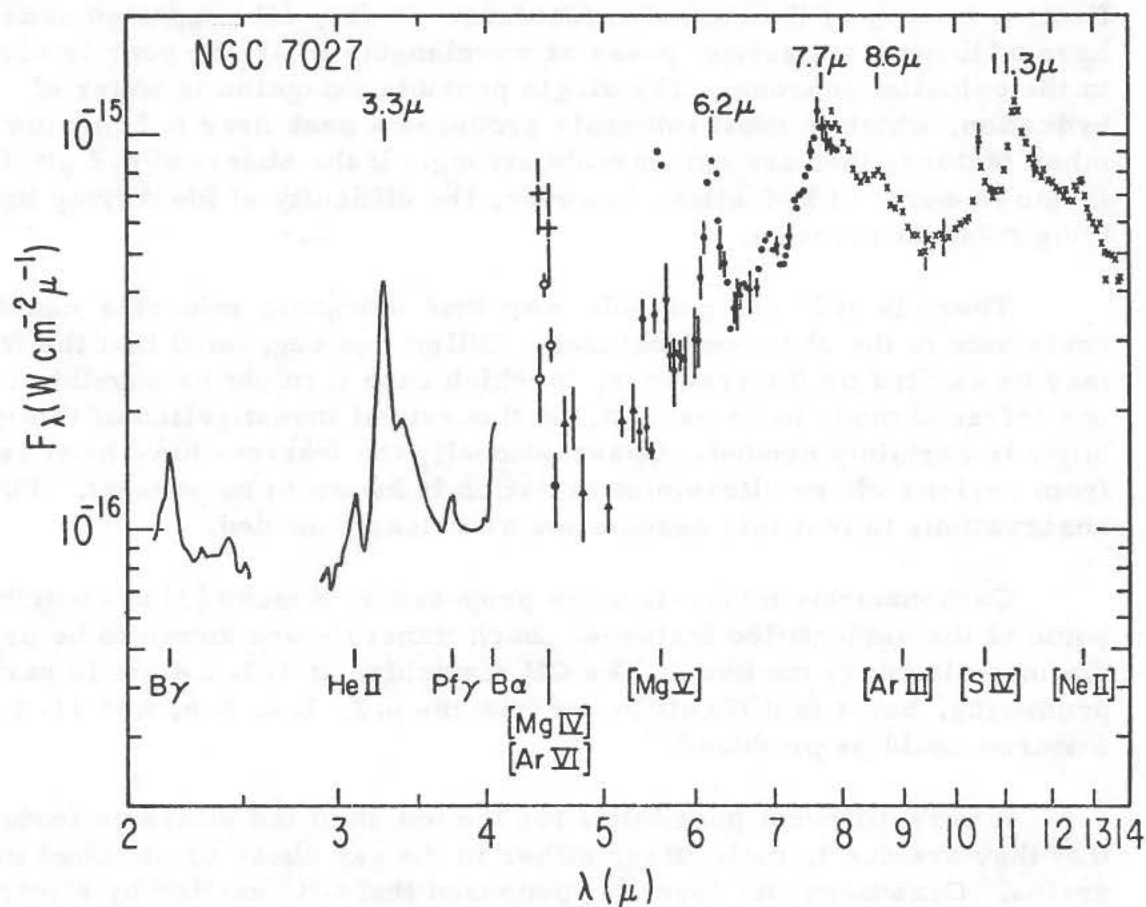


Figure 1. The 2 to 13  $\mu\text{m}$  spectrum of NGC 7027. Filled triangles have a resolution of 3%, and other points have a resolution of about 2%. Statistical uncertainties  $> 5\%$  are shown. Unidentified emission features are marked, as are the wavelengths of various atomic transitions.

## INFRARED FEATURES

Willner, S. P. et al.

the emission is due to recombination processes, while the general rise from 4 to 13  $\mu\text{m}$  is generally thought to be due to thermal dust emission. The five features whose wavelengths are marked in the figure, as well as the 3.4  $\mu\text{m}$  wing of the 3.3  $\mu\text{m}$  feature, are the unidentified features under discussion. These features occur together in many objects, including the low excitation planetary nebula BD +30° 3639, several optical H II regions such as NGC 7538, the central H II regions in the galaxy M82, and a star surrounded by dust HD 44179. In these objects, the relative strengths and shapes of the features are much the same, although the equivalent widths vary.

The earliest explanation for the emission features has been as emissivity peaks in inorganic mineral constituents of the dust. For example, Gillett, Forrest, and Merrill [2] proposed that the 11.3  $\mu\text{m}$  feature, the first to be discovered, was due to mineral carbonates. With wider spectral coverage and with the addition of measurements of inorganic compounds in our laboratory, no inorganic mineral is presently a viable identification for any of the emission features. So far, all suggested candidates have additional emissivity peaks at wavelengths where no peak is observed in the celestial sources. The single possible exception is water of hydration, which in most minerals produces a peak near 6.2  $\mu\text{m}$  and no other features that are comparably strong. If the observed 6.2  $\mu\text{m}$  feature is due to water of hydration, however, the difficulty of identifying the underlying mineral remains.

There is still one possible way that inorganic minerals could contribute to the observed features. Gillett has suggested that the features may be excited by fluorescence, in which case it might be possible for only one infrared mode to be excited. A theoretical investigation of this possibility is certainly needed. Observationally the features have been seen only from regions where ultraviolet radiation is known to be present. Further observations to test this association are clearly needed.

Carbonaceous minerals were proposed by Knacke [3] to contribute to some of the unidentified features. Such minerals are known to be present in the interplanetary medium. The CH stretching at 3.3-3.4  $\mu\text{m}$  is particularly promising, but it is difficult to see how the 6.2, 7.7, 8.6, and 11.3  $\mu\text{m}$  features could be produced.

A very different possibility for the origin of the emission features is that they are due to molecules, either in the gas phase or attached to the grains. Grasdalen and Joyce [4] proposed that  $\text{CH}^+$  excited by electron collisions is responsible for the 3.3  $\mu\text{m}$  feature, and Allamandola and Norman [5] have proposed various molecules in ice mantles on grains for all of the features. A fundamental difficulty with such proposals has been that for the estimated molecular abundances and excitation cross-sections, the expected intensity of the features is much lower than is observed. The most promising single molecule is perhaps  $\text{CH}_4$ , which has features at 3.3, 3.4, and 7.7  $\mu\text{m}$ . However, no molecule yet suggested can satisfactorily explain any of the other observed emission features.

## INFRARED FEATURES

Willner, S. P. et al.

There are two additional observations that may bear on the origin of the emission features. In the region of the Orion nebula, the features are strongest near the edge of the H II region and decrease in equivalent width nearer the center, where the silicate emission feature becomes prominent. It seems that the material responsible for the features may originate in the molecular cloud and either does not penetrate to or is destroyed in the center of the H II region.

The second observation is that at least the  $3.3\ \mu\text{m}$  feature occurs in two planetary nebulae that apparently show silicon carbide emission. The shape of the  $3.3\ \mu\text{m}$  feature is different from that in most other objects, however, in that it lacks the  $3.4\ \mu\text{m}$  wing. In one case, the  $3.3\ \mu\text{m}$  feature appears to be narrower than  $0.08\ \mu\text{m}$ , in contrast to its usual width of about  $0.15\ \mu\text{m}$ . The observations suggest, however, that at least some  $3.3\ \mu\text{m}$  features are associated with a chemical mixture where carbon is more abundant than oxygen. On the other hand, the emission features are seen in the Orion Nebula and the galaxy M82 [6], where oxygen is thought to be more abundant than carbon.

A typical spectrum having absorption features is shown in Figure 2. NGC 7538E is a compact infrared source associated with a large H II region, molecular cloud complex. The absorptions at  $3.1$ ,  $4.7$ , and  $9.7\ \mu\text{m}$  are attributed to ice, carbon monoxide, and silicates, respectively. The features at  $6.0$  and  $6.8\ \mu\text{m}$  are unidentified. Their depths are not correlated with the depth of the silicate feature but do appear to increase when the ice absorption is strong. The  $6.0$  and  $6.8\ \mu\text{m}$  features are weak or absent in the spectrum of the galactic center; this absence implies that the features are characteristic of molecular cloud material rather than of general interstellar material.

The presently most plausible identification of the  $6.0$  and  $6.8\ \mu\text{m}$  features is amorphous silicate grains. Some laboratory protosilicates, produced by Duley and McCullough [7], have two features between  $5.8$  and  $7.0\ \mu\text{m}$ , although no sample matches the exact wavelengths of the interstellar features. We do not know what molecular or crystal mode produces the features or even whether they are due to absorption or scattering. If the features are due to scattering, the increased size of grains in molecular clouds and the fact that scattering efficiency increases with increasing grain size provide a natural explanation for the presence of the features in molecular cloud material but not in the general interstellar medium. Scattering in a symmetric source, however, does not directly remove any photons. It is therefore not clear that very deep absorption features, as are indeed observed in the OH source W33A, can be produced.

## INFRARED FEATURES

Willner, S. P. et al.

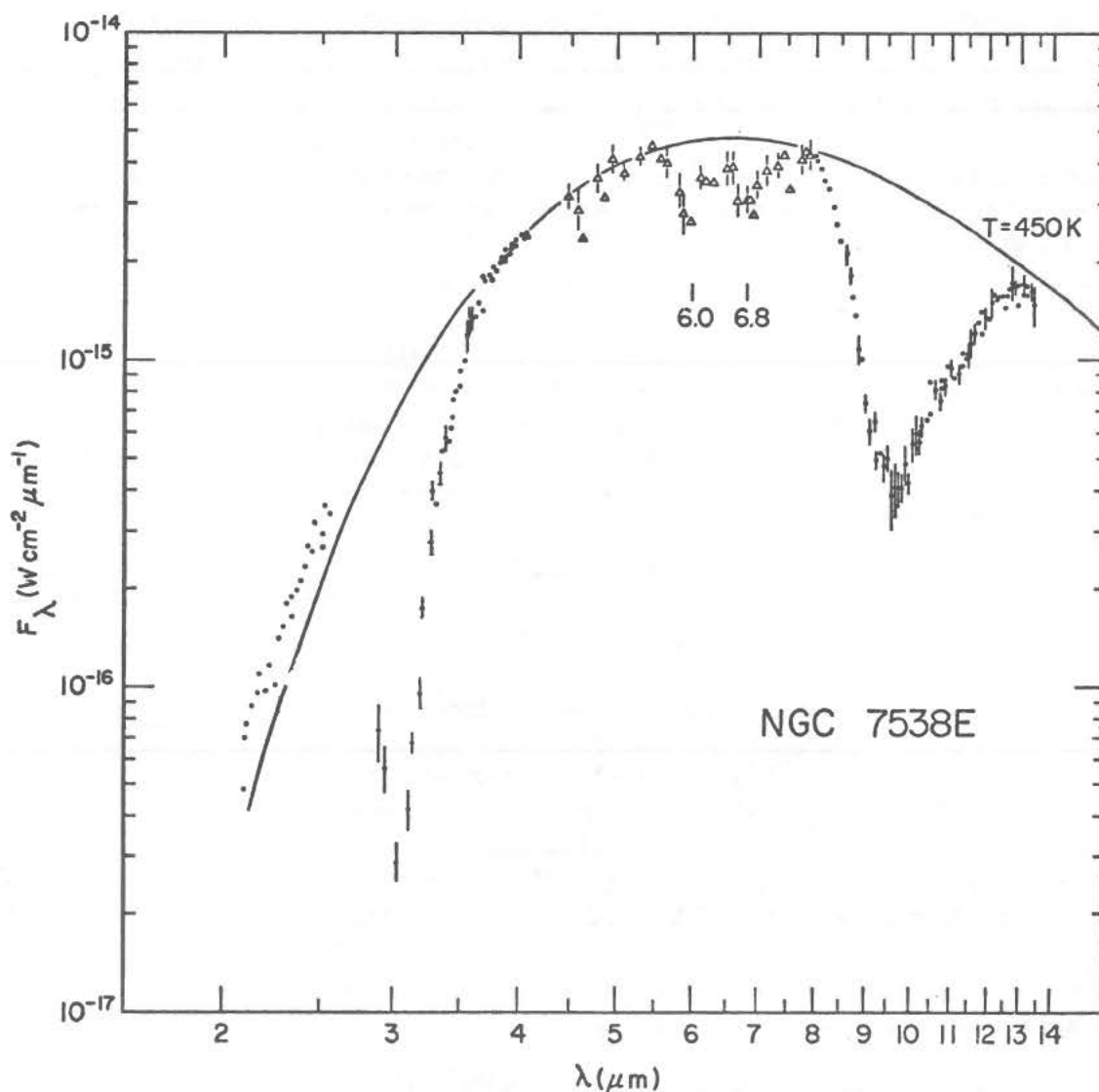


Figure 2. The 2 to 13  $\mu\text{m}$  spectrum of NGC 7538E. The spectral resolution is about 2%, and statistical uncertainties  $> 5\%$  are indicated. The line representing a 450 K blackbody is intended to show the general shape of the spectrum rather than necessarily to represent a continuum. The unidentified features at 6.0 and 6.8  $\mu\text{m}$  are marked.

A second, highly speculative, identification is molecular absorption features. The 6.0  $\mu\text{m}$  absorption would be due to stretching of C=O, while the 6.8  $\mu\text{m}$  feature would be primarily due to bending of CH<sub>2</sub>, possibly with some contribution from CH<sub>3</sub>. C=C could also contribute to the 6.0  $\mu\text{m}$  feature, but the bond intensity is too small compared to that of the CH<sub>2</sub> group for C=C to be the major absorber. One attractive feature of explaining the 6.0 and 6.8  $\mu\text{m}$  features as hydrocarbon absorptions is that CH stretching absorption would occur between 3.3 and 3.5  $\mu\text{m}$  wavelengths where there is apparent absorption that cannot easily be attributed to ice. One problem with identifying the 6.0  $\mu\text{m}$  feature as C=O is that the absorption

## INFRARED FEATURES

Willner, S. P. et al.

usually occurs at a shorter wavelength, but the characteristic frequency is lowered if the molecules are in solid or liquid form. The major problem with these identifications is that the required abundances of hydrocarbons are very large; for every 20 CO molecules indicated by the radio observations, one C=O or 5 or 10 CH<sub>2</sub> or CH<sub>3</sub> groups in hydrocarbon molecules are required.

If the various emission and absorption features can be definitely identified, they will provide new information on the composition and physical state of interstellar dust. It should be emphasized that in laboratory experiments it is necessary to measure separately the emissivities and scattering efficiencies of potential dust components, rather than only their sum. Future astronomical observations should be made of regions having a variety of temperatures, densities, and radiation fields so as to better define the conditions under which the various features occur.

## REFERENCES

1. Russell, R. W., Soifer, B. T., and Willner, S. P. 1977, Ap. J. (Letters), 217, L149.
2. Gillett, F. C., Forrest, W. J., and Merrill, K. M. 1973, Ap. J., 183, 87.
3. Knacke, R. F. 1977, Nature, 269, 132.
4. Grasdalen, G. L., and Joyce, R. R. 1976, Ap. J. (Letters), 205, L11.
5. Allamandola, L. J., and Norman, C. A. 1978, Astr. Ap., 63, L23.
6. Willner, S. P., Soifer, B. T., Russell, R. W., Joyce, R. R., and Gillett, F. C. 1977, Ap. J. (Letters), 217, L121.
7. Duley, W. W., and McCullough, J. D. 1977, Ap. J. (Letters), 211, L145.

This research was supported by NASA grant NGR 05-005-055 and NSF grant AST 76-82890.



ULTRAVIOLET SCATTERING PROPERTIES AND THE SIZE DISTRIBUTION OF INTERSTELLAR GRAINS. A. N. Witt, Ritter Observatory, The University of Toledo, Toledo, OH 43606.

Recent investigations [1,2,3,4,5,6] have established that interstellar grains possess a high scattering efficiency for far-ultraviolet light of wavelengths shortward of  $2000\text{\AA}$ . While this result itself is poorly understood in terms of the bulk optical properties of expected interstellar grain materials, it opens the way to additional studies into the nature of the particles responsible for the far-ultraviolet scattering. In particular, the scattering phase function is an observable quantity which depends primarily upon the physics of the scattering process and the size of the scattering particles and only slightly upon the chemical composition of the grains.

We have examined different astronomical scattering systems such as the galactic disk [2,4], dark nebulae immersed into the galactic radiation field [7], and reflection nebulae [6,8,9] for the purpose of deriving the wavelength dependence of the phase function asymmetry. We find that absolute values of the phase function asymmetry can be determined most reliably in the case of very dense dark clouds (globules) illuminated by the general galactic stellar radiation field. Unfortunately, observations of these objects are available only in the visible spectral region. By contrast, reflection nebulae illuminated by hot blue stars have been observed with relative ease throughout most of the visible and ultraviolet spectral regions. Uncertainties in the star-nebula geometry generally prevent the determination of absolute values of the phase function asymmetry for these systems. But, since the geometry may be considered independent of wavelength, the relative change of the phase function asymmetry can nevertheless be estimated reasonably well. Finally, the study of the diffuse galactic light arising in the disk of our galaxy by general interstellar scattering has led to rather uncertain results concerning the phase function asymmetry [2,3,10].

The best existing results indicate that the scattering phase function of interstellar grains in the visible is strongly forward directed, while a typical albedo value is 0.7. This is indicative of largely dielectric grains with sizes comparable to the wavelengths considered. Shortward of the wavelength of  $4000\text{\AA}$  there appears to be a trend to a progressively less forward throwing phase function, leading to a more nearly isotropic form in the far ultraviolet. This trend can be understood by a decreasing scattering efficiency of the wavelength sized "classical" grains and an increasing contribution from very small particles scattering nearly isotropically as we approach shorter wavelengths. These latter particles must have sizes of the order of  $100\text{\AA}$  or less with a near unit albedo in the far ultra-

## ULTRAVIOLET SCATTERING PROPERTIES

A. N. Witt

violet. This requirement is necessary to account for the observed high albedo in excess of 0.5 in the far ultraviolet and the fact that the classical grains are expected to be strong absorbers at wavelengths shortward of 2000Å.

On the basis of scattered light observations we are therefore led to the conclusion that interstellar space is populated by a bi-modal size distribution of grains, whose two components not only differ substantially in size but also fundamentally in their response to far ultraviolet photons.[11]

### REFERENCES

1. Witt, A. N. and Lillie, C. F. 1972, in "The Scientific Results from the Orbiting Astronomical Observatory (OAO-2)", ed. A. D. Code, NASA-SP310, p. 199.
2. Witt, A. N. and Lillie, C. F. 1973, Astron. and Ap., 25, 397.
3. Lillie, C. F. and Witt, A. N. 1973, in "Interstellar Dust and Related Topics", (IAU Symposium No. 52), ed. J. M. Greenberg and H. C. van de Hulst (Dordrecht: Reidel), p. 115.
4. Lillie, C. F. and Witt, A. N. 1976, Ap. J., 208, 64.
5. Carruthers, G. R. and Opal, C. G. 1977, Ap. J. Lett., 212 L27.
6. Andriesse, C. D., Piersma, Th. R., and Witt, A. N. 1977, Astron. and Ap., 54, 841.
7. FitzGerald, M. P., Stephens, T. C., and Witt, A. N. 1976, Ap. J., 208, 709.
8. Witt, A. N. 1977, Publ. Astr. Soc. Pac., 89, 750.
9. Witt, A. N. and Lillie, C. F. 1978, Ap. J., 212, 909.
10. Henry, R. C., Anderson, R., Feldman, P. D., and Fastie, W. G. 1978, Ap. J., 222, 902.
11. Witt, A. N. 1973, in "Interstellar Dust and Related Topics", ed. J. M. Greenberg and H. C. van de Hulst (Dordrecht: Reidel) p. 53.

## SUBJECT INDEX\*

- Activation energy 4, 34
- Albedo 70
- Allende meteorite 38, 59
- Amorphous grains 56
- Amorphous ice grains 53
- Amorphous silicates 51
- Amorphous structure 34
- Analogues to cosmic dust 30
- Association reactions 23
- Ca- Al-rich inclusions 59
- Carbonaceous chondrite 30, 59
- Chains of submicron particles 30, 45
- Chemistry of interstellar grains 20
- Chromium 38
- Circumstellar dust 43
- Classical nucleation theory 50
- Clustering 30, 45
- Comets 51
- Computer simulation 50
- Condensation 4, 14, 23, 34, 38, 50
- Condensation experiment 30
- Condensation kinetics 17, 30
- Condensation of chromium 38
- Condensation of magnesium 38
- Condensation of silicates 30
- Condensation of silicon 38
- Condensation parameters 4
- Condensation temperature 14
- Condensation theory 17
- Cosmic dust 42, 59
- Cosmic grains 42, 59
- Cosmogony 42
- Critical cluster 34, 50
- Crystalline structure 34
- Dark interstellar clouds 4
- Depletion in interstellar medium 9, 20
- Diffusion phenomena 4
- Dust 25, 51, 65
- Dust cloud 4, 14
- Dust formation 43
- Early solar system 14, 30, 40, 45
- Electric discharge 25
- Electrostatic disruption of grains 42
- Equilibrium condensation 59
- Excitation and ionization effects 4
- Fine particle 30, 34, 45
- Fine-grained inclusions 59
- Fluid dynamics 40
- Fractionation 38
- Gas condensation 12
- Gas phase 34
- Grain dynamics 40
- Grain formation 40
- Grain growth 9, 34
- Grain sputtering 40
- H<sub>2</sub> recombination 53, 64
- Ices 43
- Infrared 51, 56
- Infrared 10 $\mu$  absorption 51
- Infrared 10 $\mu$  emission 51
- Infrared 10 $\mu$  feature 51, 56
- Infrared emission bands 43
- Infrared properties of grains 43
- Infrared spectra 20, 25
- Interstellar clouds 23
- Interstellar dust 20, 43, 56
- Interstellar grains 1, 18, 64, 70
- Interstellar matter 12
- Isotope fractionation 4, 9, 40, 45
- Isotopic anomalies 4, 40

\*Pagination refers to first page of paper in which subject is cited.

- Kinetics 17, 34
- Laboratory astrophysics 12
- Laboratory condensate 12, 17, 25, 30, 56
- Low and high supersaturation 30
- Magnesium 38
- Magneto-gravitational capture 42
- Magnetospheres 42
- Mass loss 18, 43
- Matrix 59
- Metastable phase 30
- Meteorite 4, 14, 38
  - isotopic anomalies 4, 40
- Molecular hydrogen 53, 64
- Molecular synthesis 23, 25
- Molecule growth 4, 23, 50
- Molecules 65
- Multiphase grains 30
- Nebulae 65
- Necklace structure 45, 56
- Non-linear fractionation 4
- Nova ejecta 9
- Nucleation 9, 17, 34
  - experiment 17, 34
  - kinetics 17, 50
  - theory 9, 18
- Olivine 38
- Opacity 4, 14
- Organic dust 25
- Phase function 70
- Phase transformation 34
- Planetary nebulae 18
- Plasmas 42
- Platinum metals 59
- Porosity 45
- Primordial solar nebula 14, 30, 45
- Rayleigh-Taylor instabilities 40
- Refractory elements 38
- Rims 59
- Satellites 42
- Scattering properties 70
- Silicates 43, 51, 56
- Silicon 38
- Size distribution 45, 70
- Solar nebula 14, 30, 45
- Source medium 4
- Spectra 25, 56, 65
- Sputtering 12
- Stellar mass loss 18, 43
- Substrates 12, 34
- Supernova ejecta 9, 40
- Surface chemistry 20
- Surface reactions 53, 64
- Synthesis 25
- Temperature fluctuations 1
- Temperature parameters 4, 14
- Thermal disequilibrium 14
- Thermal equilibrium 14
- Turbulence 40
- Ultraviolet spectra 25





## AUTHOR INDEX\*

Aannestad, P. A. 1  
 Arrhenius, G. 4, 14  
 Berne, B. J. 50  
 Clayton, D. D. 9  
 Day, K. L. 12  
 De, B. R. 14  
 Donn, B. 17  
 Draine, B. T. 18  
 Duley, W. W. 20  
 Falk, S. W. 40  
 Herbst, E. 23  
 Hunter, D. A. 64  
 Kamijo, F. 45  
 Kenyon, S. J. 1  
 Khare, B. N. 25  
 Kothari, B. K. 30  
 Krikorian, E. 34  
 Larimer, J. W. 38  
 Margolis, S. H. 40  
 MacLean, S. 20  
 McCrumb, J. L. 4  
 Mendis, D. A. 42  
 Merrill, K. M. 43  
 Millar, T. J. 20  
 Nakada, Y. 45  
 Onaka, T. 45  
 Puetter, R. C. 65  
 Rao, M. 50  
 Rose, L. A. 51  
 Russell, R. W. 65  
 Sagan, C. 25  
 Smoluchowski, R. 53  
 Sneed, R. J. 34  
 Soifer, B. T. 65  
 Stephens, J. R. 30, 56  
 Wark, D. A. 59  
 Watson, W. D. 64  
 Williams, D. A. 20  
 Willner, S. P. 65  
 Witt, A. N. 70

\*Pagination refers to first page of paper in which author is cited.



National Aeronautics and  
Space Administration

**Lyndon B. Johnson Space Center**  
Houston, Texas 77058